Volume 2 *June, 1932* *Number 6*

PHYSICS

Electronic Devices as Aids to Research

By A. W. HULL
General Electric Company, Schenectady, New York

(Received March 21, 1932)

IN THE first issue of Electronics (April, 1930), the editor, O. H. Caldwell, lists 175 industrial applications of electron tubes. In the same number, Mr. J. W. Horton, chief engineer of General Radio Company, prefaces his treatment of *Electron Tubes in Scientific Measurements* with the statement: "It is probable that the entire issue of this magazine for one year would be required merely to outline the uses to which the vacuum tube has been put."

I shall not attempt such an outline, but shall rather try to describe some of the most recent improvements in these devices.

As a background, however, a brief summary of the scope of *scientific* applications of electronic devices may be permitted.

ELECTRONIC TOOLS AND THEIR FUNCTIONS

The most useful electronic devices, from the standpoint of research, are five in number, *viz.:* the x-ray tube; the cathode-ray oscillograph; the photoelectric tube; the Pliotron; and the Thyratron.[1] In addition, many scientific uses are found for the Kenotron rectifier, as rectifier and current limiting device; the magnetron, for measuring magnetic fields and as generator of ultra high-frequencies; the dynatron, as variable frequency oscillator and for measurement of power losses; glow tubes of various types, especially the grid-glow tube,[2] for use as rectifiers, regulators, relays, and timing devices; the Lenard-Coolidge cathode-ray tube, for experiments in chemical dissociation, and for fluorescence studies; *tungar* and mercury arc rectifiers; and internally photosensitive devices, such as selenium, copper oxide, and *thalofide.*

The main function of these electronic devices, in aiding research, is to make possible the measurement of *smaller things* than could be measured before, with *less disturbance,* by the measuring rod, of the thing measured. The uncertainty principle teaches that the ultimate limit of smallness that can be observed is reached, when the quantity to be measured is smaller than

[1] A. W. Hull and I. Langmuir, Proc. Nat. Acad. Sci. **51,** 218 (1929); A. W. Hull, Gen. Elec. Rev. **32,** 213, 390 (1929).

[2] D. D. Knowles, Electric Journal **27,** 116, 232 (1930).

the disturbance caused by the application of the measuring means. Electronic devices allow us to approach this ideal limit by supplying us with the lightest known measuring agents, electrons and photons.

Thus, electronic devices enable us to measure, without disturbing them, *smaller voltages*, *smaller currents*, *smaller distances*, *smaller times*, *smaller sounds*, and *smaller light*. Examples of small voltages include the transient voltages due to heart beat and nerve reaction; of small currents, the ionization due to a single ion or photon; of small distance, the separation of atoms in a molecule; of small time, the breakdown of a spark gap in air or vacuum, which can be timed to 1/100 microsecond by the cathode-ray oscillograph; of small sounds, speech transients and the noise of machines; of small light, the radiation from a distant star.

Typical uses of electron tubes

The extent to which these new measuring devices have expanded the field of scientific research is very impressive. The following examples, from different fields, will show what a large fraction of present day research not only uses these tools, but could not exist without them.

1. Communication.—Amplifiers, carrier-current, and radio have given birth to a new art and a new science of communication.

2. Acoustics.—A dead science has been reborn, due partly to the interest in better reproduction of music and speech which has been created by radio, film records, and electrical disk recording; and partly to the new possibilities, created by vacuum devices, for studying the structure of speech and the physiology of hearing. Thus, the *new acoustics* may be said literally to owe its life to vacuum tubes.

3. Crystal analysis.—This is a new science, born of the x-ray tube. It employs many scientists.

4. Molecular structure.—A large group of physicists are busy in this field with various electronic tools, measuring the separation of atoms in gases and liquids by means of x-rays, and measuring dipole moments by the variations in energy absorption and dielectric constant at high frequencies. These jobs were created by electronic tools.

5. Electrical engineering.—The cathode-ray oscillograph has opened up a new field of investigation in rapidly-occurring electrical phenomena, such as lightning, transient voltages in transformers, and the nature and mechanism of breakdown of spark gaps in air and in vacuum. Harmonics in alternating currents are studied by the heterodyne electron-tube oscillator; synchronization by the thyratron stroboscope; electrical distribution by *miniature* distribution systems using electron tube amplifiers; the nature of magnetism by the study of *Barkhausen* discontinuities, with the help of electronic tools.

6. Mechanical engineering.—The study of machine noises and vibrations offers a new field for the investigation of rotating machines. In this there is a promise of compensation; *viz.*, that the same devices, which have given us radio and so contributed to the noise and confusion of life, may in the end

produce quieter living conditions by eliminating the unnecessary noises of machinery.

7. Metallurgy.—X-ray crystal analysis is revolutionizing this science by furnishing an instrument for studying the structure and nature of alloys, the mechanism of inelastic deformation, and the causes of hardening. High voltage x-rays reveal faults in castings and welds, cathode rays the impurities in minerals, electron waves the structure of surfaces.

8. Oceanography.—Echo depth measurement opens a new field of study of the ocean bottom, for navigation and for geological science. Similar echoes and transmission times are used in the study of the earth's crust.

9. Biology.—X-rays are used for the study of anatomy, of experimental cancer, and of chromosome cross-over; high-frequency *fever* waves for studying the benign effects of fever; electron-tube amplifiers for the quantitative study of nerve and muscle response to stimuli; high-frequency *electric knives* for bloodless surgery.

New Electronic Devices

Among recent developments in electronic devices, three are of especial interest to research workers in physics and optics, and the remainder of this paper will be devoted to them. They are:—

1. Red-sensitive photoelectric tubes.
2. Special vacuum tube amplifiers for small currents and voltages.
3. The Thyratron.

Red-sensitive phototubes

Red-sensitive tubes are desirable for radiation measurements from several standpoints. In the first place, they are much more sensitive to the light of a tungsten filament, and hence more suited to a large variety of measurements and applications. The best caesium oxide tubes of today are approximately 100 times as sensitive to tungsten lamps as the best tubes available five years ago. Secondly, red tubes are more easily adjusted by filters to the visual sensitivity curve, hence useful for photometry. The third and most important reason is that their response covers the whole visible spectrum, from extreme ultraviolet to the limit of glass transmission in the infrared, which makes them suitable for spectrophotometry. The most recent caesium tubes are reported to be sensitive beyond 15,000A, the tests having been limited by the transparency of the glass.

Progress in phototube development.—The most electropositive pure metal caesium, has its long wave-length threshold at about 6000A. The only pure metal which can be expected to respond to longer wave-lengths is the newly discovered hekacaesium. It has been found, however, that this limit can be exceeded by properly *impurifying* the surface, making it a two-component surface. Such a treatment is known to increase thermionic emission.[3] Thus, a considerable increase in red photosensitiveness is attained by depositing

[3] I. Langmuir and K. H. Kingdon, Phys. Rev., **22,** 375 (1923); Proc. Roy. Soc. **A107,** 68 (1925); Science **57,** 58 (1923).

the alkali as a monatomic film on another metal.[4] It is worth noting that these thin film experiments, while not leading to a practical tube, have had a by-product which is perhaps more important than a new tube, namely, the discovery that the photoelectric effect is determined by the electric *intensity* at the metal surface; and that when expressed in terms of this intensity, rather than incident or absorbed energy, the difference between *normal* and *selective* photoelectric effect disappears.[5]

"Staining" the alkali surface with red-sensitizing dyes greatly increases the red-sensitiveness.[6] A large number of inorganic and organic substances have been found to be effective, especially sulphur compounds such as sodium bisulphite, and organic dyes such as alizarine blue and kryptocyanine. Such *treatment* of the alkali surface increases the response range to 10,000A. The *potassium hydride* tubes, first made by Elster and Geitel, and subsequently by many investigators and manufacturers, in which a potassium surface is sensitized by a glow discharge in hydrogen, belong to this class. It is probable that the final state of the surface under these treatments is similar to that of the tubes next to be described, with the important exception that the *treated surface* tubes contain free alkali metal, which tends to make the sensitive condition unstable and temporary.

The third and best method, to date, of increasing red-sensitiveness, is to deposit a thin *partial* layer of alkali metal on an *electronegative* substance, such as oxygen or a metallic oxide. The best red-sensitive tubes thus far produced have a partial monatomic film of *caesium* on *oxidized* silver.[7] An important part of the process of making these tubes is the removal of excess caesium, either by distilling it out of the bulb, or by firmly *fixing* it on some appropriate substance within the bulb. Without this precaution, it is difficult to maintain the optimum thickness of the photoelectric caesium layer, which, as in the case of thermionic emission, is less than one complete monatomic layer. The photosensitive caesium atoms are believed to be adsorbed on the oxygen, which, in turn, is adsorbed on the silver,[8] or adsorbed on caesium oxide,[9] or adsorbed on a combination of caesium oxide and silver-caesium alloy.[10] In view of these uncertainties in theorys it is not surprising that the practical formation of these surfaces is still an art, as evidenced by the following record of improvement in sensitivity for the last three years.

Sensitivity of "caesium oxide" phototubes.—In 1928, when caesium oxide photoelectric tubes were first made, a vacuum sensitivity of 0.7 microamperes per lumen was considered good,[8] using as light source a tungsten lamp at color temperature 2850° K. This sensitivity was about equal to that of the best potassium hydride tubes at that time. In 1929, Koller[11] reported

[4] H. E. Ives, Astrophys. Journal **60,** 209 (1924).
[5] H. E. Ives, Phys. Rev. **38,** 1209, 1477 (1931).
[6] A. R. Olpin, Phys. Rev. **36,** 251 (1930).
[7] K. Bainbridge, (Unpublished data), British Pat. No. 303476.
[8] L. R. Koller, Gen. Elec. Rev. **31,** 476 (1928).
[9] J. H. DeBoer and M. C. Teves, Zeits. f. Physik **65,** 489 (1930).
[10] N. R. Campbell, Phil. Mag. **12,** 173 (1931).
[11] L. R. Koller, Phys. Rev. **33,** 1082A (1929).

a sensitivity of 5 microamperes per lumen, and in 1930,[12] 18 microamperes per lumen. Zworykin and Wilson[13] in 1930 gave 25 microamperes per lumen as the limit of vacuum sensitivity for caesium-oxygen-silver tubes, while for caesium-on-magnesium tubes they reported a sensitivity of 2 microamperes per lumen. In 1931, Campbell[10] reported a maximum vacuum sensitivity as high as 49 amperes per lumen for a laboratory tube, and from 10 to 12 microamperes per lumen for factory made tubes. Factory made General Electric vacuum type caesium phototubes had, in 1931, a rated sensitivity greater than 4 microamperes per lumen, with individual values as high as 40 microamperes per lumen. Late in 1931, Teves[14] reported a sensitivity of 20 to 30 microamperes per lumen for regular factory made tubes and as high as 65 microamperes per lumen for several specimens, with a maximum long wave-length limit of 1.4μ; while Asao[15] has obtained a sensitivity of 60 microamperes per lumen. Recently DeBoer and Teves[16] have reported caesium oxide tubes with a vacuum sensitivity of 120 microamperes per lumen, and wave-length sensitivity extending beyond the range of transparency of their glass.

All the values given above refer to vacuum type caesium-oxygen-silver tubes, tested with gas-filled tungsten lamps operated at color temperature between 2680°K and 2870°K. For the stained tubes, Olpin[6] reports a sensitivity of 7 microamperes per lumen for treated sodium surfaces and "much higher sensitivity for caesium." All of these tubes can be improved in sensitivity by a factor of about 10 by *gas amplification*, that is, by the addition of a small amount of ionizable inert gas, preferably argon, and operation at a voltage just below the glow-potential. Such amplification by ionization, however, introduces instability, non-linearity, high *noise level*, and time lag, and is not in general to be recommended for measurement purposes.

From these references it is apparent that the total sensitivity of phototubes to light from a tungsten lamp has been increased about one hundred fold in the last three years. This has a very important bearing upon the usefulness of phototubes for measurement purposes. Illustrations of such usefulness are: sound analysis and reproduction, optical and electrical measurements, and numerous industrial control applications.

Theoretical predictions.—Theories of the photoelectric effect admit the possibility of still further increase in sensitiveness and still further extension into the infrared. The only quantitative theory thus far evolved[17] applies only to pure metals, but appears to give complete agreement with experimental measurements.[18] Photoelectric theory is thus on a par with thermionic theory.

[12] L. R. Koller, Phys. Rev. **36,** 1639 (1930).

[13] Zworykin and Wilson, *Photocells and their Applications,* John Wiley and Sons, 1930.

[14] M. C. Teves, Zeits. f. tech. Physik **12,** 556 (1931).

[15] S. Asao, Physics, **2,** 12 (1932); S. Asao and M. Suzuki, Proc. Inst. Rad. Eng. **19,** 655 (1931).

[16] DeBoer and Teves, (Private communication from Dr. G. Holst, to be published soon in Zeits. f. Physik.)

[17] R. H. Fowler, Phys. Rev. **38,** 45 (1931).

[18] L. A. DuBridge, Phys. Rev. **39,** 108 (1932).

The best known theory of composite surfaces regards the emission as coming from the base metal under the influence of the strong electrostatic field due to the adsorbed electropositive atoms.[19] Recent measurements[20] upon the *selective* photoemission from partial monatomic films of caesium on silver have led to the conclusion that the emission must come from the caesium atoms themselves, rather than from the underlying surface. A theory, developed by Fowler,[21] correlates the de Broglie wave-length of the escaping electrons with the distance between the planes of atoms in the surface layers. Olpin,[22] by an extension of this theory, was able to account quantitatively for the position of the maximum in the wave-length sensitivity of alkali hydrides, oxides, and sulfides, but the agreement which he obtained has been criticized by Zachariasen[23] as fortuitous. DeBoer and Teves[24] derive the photoelectric work function for adsorbed films from that of the atoms in gas form, by equating the work of ionizing the free atom (ionizing potential) to

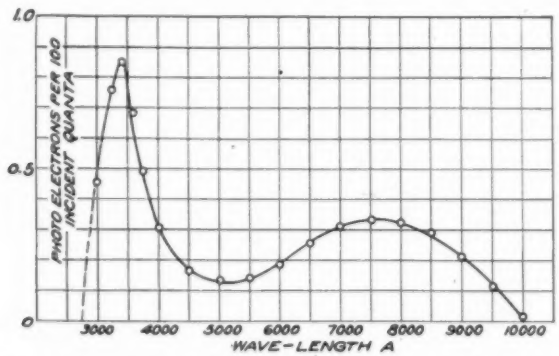

Fig. 1. Quantum efficiency of typical Cs-O-Ag phototube.

that of a three-step process, consisting of adsorption of the atom, photoelectric emission, and evaporation of the resulting adsorbed ion. The photoelectric work function of the adsorbed atom is thus equal to the ionizing potential minus the difference between the heats of evaporation of atom and ion.

From all these points of view it may be concluded that the photoelectric work function should be lower the greater the distance between the adsorbed photosensitive atom and the underlying conductor.

A measure of the ultimate possible sensitivity is the quantum efficiency, that is, the number of photoelectrons per photon. Teves[14] gives a maximum efficiency of "one electron for ten quanta," for a tube having a total sensitivity of 65 microamperes per lumen at color temperature 2680°K. The calculation

[19] I. Langmuir, Gen. Elec. Rev. **23,** 504 (1920); J. A. Becker, Phys. Rev. **28,** 341 (1926); J. W. Becker and R. W. Sears, Phys. Rev. **38,** 2193 (1931).

[20] H. E. Ives and H. B. Briggs, Phys. Rev. **38,** 1477 (1931).

[21] R. H. Fowler, Proc. Roy. Soc. **A128,** 123 (1930).

[22] A. R. Olpin, Phys. Rev. **38,** 1745 (1931).

[23] W. H. Zachariasen, Phys. Rev. **38,** 2290 (1931).

[24] DeBoer and Teves, Zeits. f. Physik. **73,** 192 (1931).

is presumably made on the basis of absorbed energy rather than incident energy. Fig. 1, kindly prepared by Dr. Koller, gives the quantum efficiency per unit *incident* energy, for a Cs-O-Ag tube having a total sensitivity of 33 microamperes per lumen at 2870°K. It is seen that the maximum efficiency is approximately 1 percent, that is, one photoelectron for 100 incident quanta.

Use of phototubes for photometric measurements.—A typical sensitivity curve for a Cs-O-Ag phototube is shown in Fig. 2. The double maximum, in the blue and red respectively, is characteristic of these tubes. For comparison, the characteristic of pure Na (in quartz), pure Cs, and a typical potassium hydride tube are shown in the same figure. It would appear at first sight that the red Cs-O-Ag tube with its double maximum should be less suited to photometric measurements than the other types of tubes, since it departs much more from the shape of the visual sensitivity curve. The important

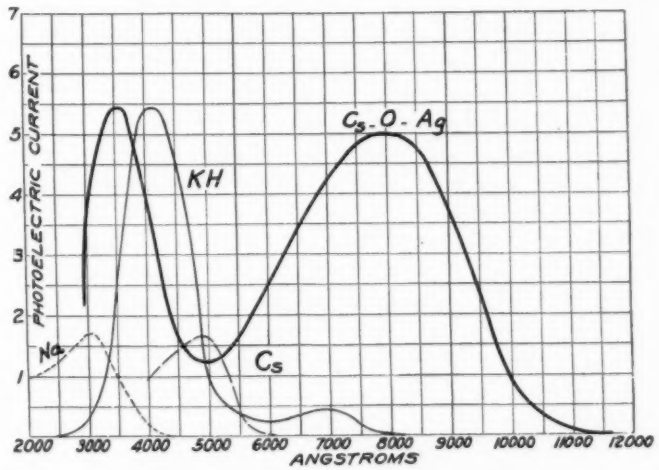

Fig. 2. Spectral sensitivity curve of typical Cs-O-Ag phototube, compared with pure Na, pure Cs, and a typical KH tube.

fact, however, is that it responds with considerable sensitivity to all the wavelengths of the visual range. Fig. 3[25] shows, in curve I, the characteristic sensitivity curve of the Cs-O-Ag tube, in curve II the sensitivity curve of the eye, and in curve III the ratio of these two. This ratio is the ideal filter necessary to make the tube sensitivity the same as visual sensitivity. Fig. 4 shows this ideal filter curve (dashed) compared with the observed transmission of a two element filter of inorganic salts, *viz.*, a mixture of 1/100 normal potassium bichromate, and 1.5 normal copper chloride. It is believed that this filter could be used, without appreciably greater errors than shown in Fig. 4, for the standard run of commercial Cs-O-Ag phototubes.

The use of photoelectric photometric methods greatly increases the accuracy as well as the ease of photometric measurements. Fig. 5[26] shows a

[25] Arthur M. Lockie, thesis, R.P.I. June 1931 (to be published soon).

[26] Dudding and Winch, Accuracy of Commercial Photometry, Proc. In't'l. Illumination Congress at Glasgow, 1931.

curve of relative errors of photoelectric and visual photometry. The photoelectric errors shown, which are approximately half as great as the visual errors, are stated to be due principally to errors in reading the lamp voltage.

Spectrophotometry offers a more important field for red-sensitive tubes. A recent review[27] of the possible errors in such applications shows that the development of the photoelectric tube is still far from the point where it can be used as a calibrated instrument of definite and predictable spectral sensitivity. A method recently developed by A. C. Hardy[28] avoids this difficulty,

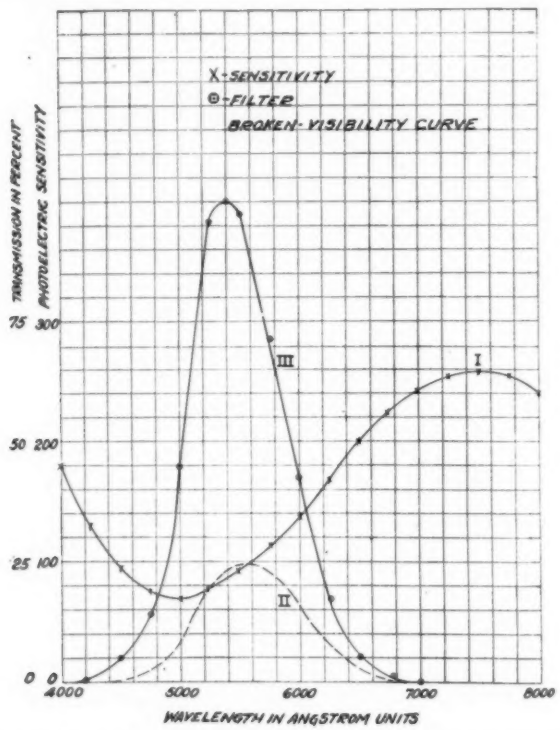

Fig. 3. Ideal filter for Cs-O-Ag phototube. I. Sensitivity curve of Cs-O-Ag phototube. II. Sensitivity curve of eye. III. Ideal filter needed to reduce I to II.

and requires only that the tube should respond with a measurable intensity throughout the whole spectrum. Hardy's method is to expose the tube in rapid succession first to the light to be measured and then to a standard source. The two sources may then be either compared directly or resolved by a prism and the separate wave-lengths compared. In a completed instrument of this type, it is possible to analyze the complete spectral color distribution of a sample in less than one minute, with an accuracy equal to the best photometric determinations that have ever been made. It is stated[29] that indi-

[27] H. E. Ives and E. F. Kingsbury, Jour. Op. Soc. Am. **21,** 541 (1931).

[28] A. C. Hardy, Jour. Op. Soc. Am. **18,** 96 (1929).

[29] A. C. Hardy and O. W. Pineo, paper presented to Am. Phys. Soc., Cambridge, Mass. Feb. 25, 1932.

vidual readings in the comparison of two sources with this instrument can be made with an accuracy of 0.035 percent.

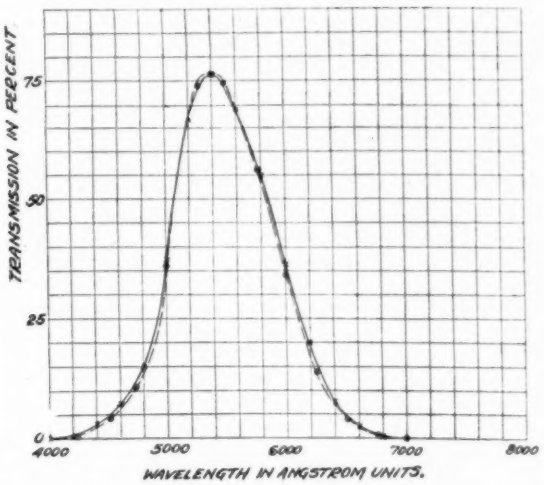

Fig. 4. Transmission of two-element inorganic filter prescribed for Cs-O-Ag phototube. Dashed curve—ideal filter characteristic (curve III of Fig. 2). Full curve—Observed transmission of N/100 potassium bichromate +1.5 N copper chloride.

Fig. 6 shows schematically Hardy's color analyzer as applied for automatic registration. "The operation of this instrument may be briefly described

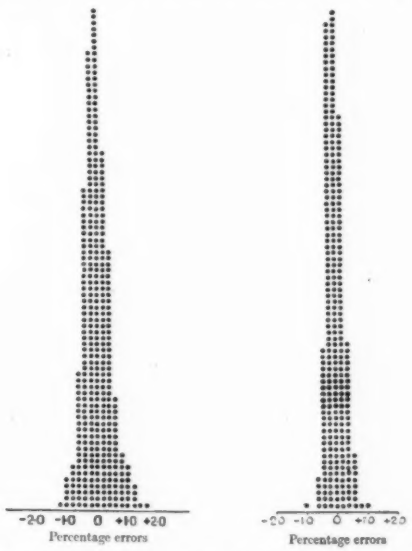

Fig. 5. Comparison of visual and photoelectric photometry. Left—Repetition accuracy of precision visual photometer (mean of two observers). Right—Repetition accuracy of photoelectric photometer (used in precision laboratory).

as follows: the specimen and a (standard white) surface of magnesium carbonate are illuminated from opposite sides of a ribbon filament tungsten

lamp. Beams of light from the specimen and from the magnesium carbonate standard are alternately admitted, by a rotating disk, to the slit of a dispersing system. Narrow bands of each of the spectra thus formed fall successively on a photoelectric tube, and cause a pulsating current in the tube circuit when the two beams are of unequal intensity. This current is amplified by Pliotron tubes and the alternating component is applied to the field coils of a small motor, the armature being supplied from an independent source of the same frequency. With this arrangement, the armature rotates in one direction when the beam from the specimen is more intense and in the opposite direction when the beam from the standard is more intense. When the intensities are equal, the field current ceases and the motor stops. By causing the motor to control a diaphragm which varies the illumination

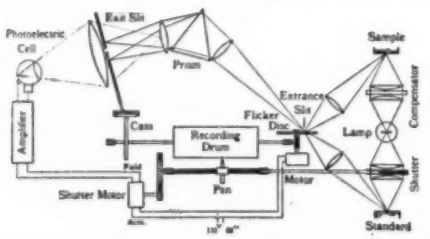

Fig. 6. Schematic diagram of spectrophotometric color analyzer, by A. C. Hardy.

on the magnesium carbonate, the intensities of the two beams are automatically balanced. A pen operating on a rotating drum records the position of this diaphragm while the rotation of the drum changes the wave-length of the spectral band admitted to the photoelectric tube. In this way, a complete spectrophotoelectric curve for the entire visible spectrum is traced in approximately thirty seconds."

Another important application is stellar photometry. The photoelectric photometer recently installed by Stebbins[30] on the 40-inch refractor at the Yerkes Observatory, using the best (Kunz) potassium-hydride-in-quartz tube available, is able to measure stars as faint as the ninth magnitude. The current given by a ninth magnitude star is 10^{-13} amperes, which can be measured to 1 percent accuracy with the available electrometer sensitivity of 10^{-15} amperes.* Stebbins states[30] that the "particular advantage of the photoelectric tubes is that conditions of seeing have no influence on the

[30] Joel Stebbins, Astrophys. Journal **74**, 289 (1931).

* Since this paper was written, the following letter from Dr. Stebbins, dated April 14, 1932, shows still further progress:

"A few weeks ago I wrote you saying that we hoped soon to be measuring stars with a photoelectric cell and a Pliotron tube. I am now glad to say that during the past week we have tried out such a set-up, and somewhat to my surprise we have attained a sensitivity four times greater than with the previous combination of cell and the electrometer. We are now getting measures of stars which were formerly quite out of reach and a new field of work has been opened for us with our telescope.

"The trick that did the work is simply to evacuate the chamber containing cell and tube, which seems to eliminate a large number of the irregularities. The limit of detection is about 10^{-16} amperes which corresponds roughly to photoelectric current from a star of magnitude 14."

measures of stars." If, in addition, tubes with a sufficient range of color sensitivity can be used, the separation of stars by color, by the use of appropriate filters, will greatly extend the field of observation. It appears probable that the red-sensitive tubes, whose development has been described, could be made free from insulation leakage (see next section), and the limit of sensitivity would be the thermionic emission, which is of the order of 10^{-12} amperes at 0°C. Thus, to use these tubes with measuring devices having a sensitivity of 10^{-17} amperes, as described in the next section, it would be necessary to cool the tube to −60°C.

Special vacuum tube amplifiers for small currents and voltages

Pliotrons for measuring small currents.—Attempts to use Pliotron tubes for small current measurements have been published from time to time by

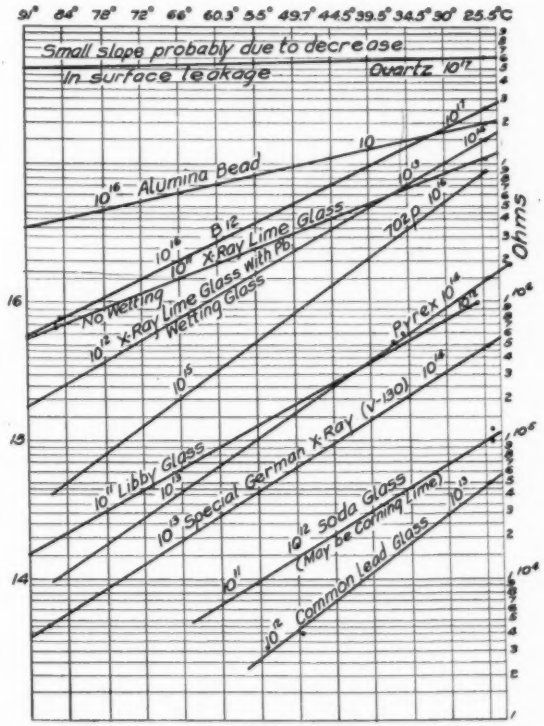

Fig. 7. Resistance of typical dry insulators, of dimensions shown, as function of temperature.

various workers. Effort has usually been concentrated on avoiding *insulation leakage* and *ionization* of residual gas. The first is usually obviated by the use of a quartz stem, or by enclosing the glass stem in a moisture proof envelope containing drying material with amber lead-in; the second, by operating below the ionizing potential of ordinary gases.

About five years ago investigations were started in the Research Laboratory to determine the nature of additional sources of leakage. Dr. L. P. Smith, who spent a summer in the laboratory, was able to show that the largest

residual source of leakage was positive ion emission by the hot cathode,[31] which is of the order of 10^{-11} amperes for a well aged tungsten filament at 2100°K. During the next summer, Dr. Howard L. Bronson investigated insulation leakage. He found, contrary to expectation, that the better commercial glasses, such as Corning B-12 lead glass, are satisfactory insulators for the most sensitive "electrometer" tubes, provided the glass is clean and properly polarized.

Cleanness is paramount. Quartz insulators, mounted in vacuum, leak badly if they have been touched with the fingers before mounting. Fig. 7

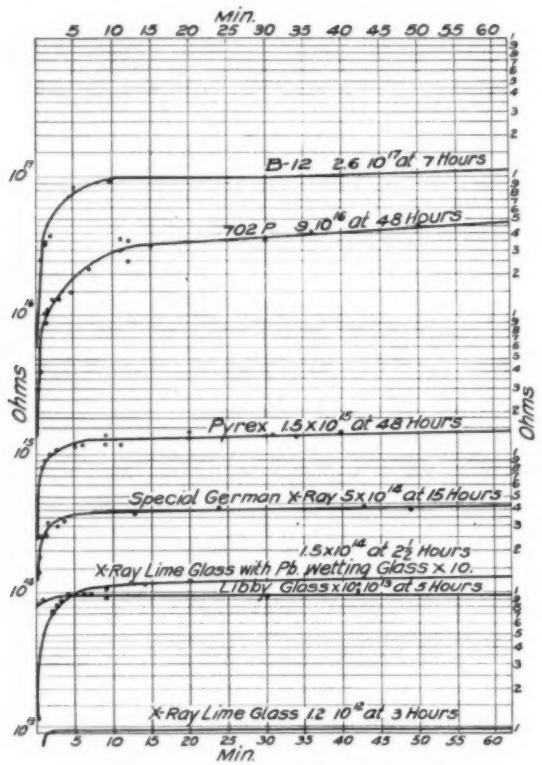
Min.
5 10 15 20 25 30 35 40 45 50 55 60
B-12 2.6 10^17 at 7 Hours
702 P 9.10^16 at 48 Hours
Pyrex 1.5x10^15 at 48 Hours
Special German X-Ray 5x10^14 at 15 Hours
1.5x10^14 at 2½ Hours
X-Ray Lime Glass with Pb. wetting Glass X 10.
Libby Glass x10; 10^13 at 5 Hours
X-Ray Lime Glass 1.2 10^12 at 3 Hours
Ohms
Ohms
Min.

Fig. 8. Resistance of dry glass as function of time after applying voltage. Applied voltage 115 volts.

gives the resistance of a few typical glasses, and samples of quartz and alumina, in clean, dry condition, as a function of temperature.

Polarizing is accomplished by impressing the operating voltage upon the glass some hours before measurements are to be made. The need for this is shown in Fig. 8, which gives the resistance as a function of time after voltage is applied. It is seen that the rate of change of resistance, which is the leakage current, is enormous for the first 10 minutes, and is appreciable after an hour.

Bronson found that clean glass could be used, even in humid summer weather, without serious leakage if its temperature were raised a few degrees

[31] L. P. Smith, Phys. Rev. **35**, 381 (1930).

above ambient. This is shown in Fig. 9, which gives the resistance as a function of temperature, on a humid day. It will be noted that in the sample marked "Libby," which is a high melting steam-gauge tubing, the volume conductivity predominates over surface leakage, so that any increase of temperature decreases the total resistance. Corning 702 P (nonex) and Pyrex show an optimum temperature, for the given dimensions, of 20° and 10° respectively, above ambient. Quartz, with negligible volume leakage, is better the higher the temperature.

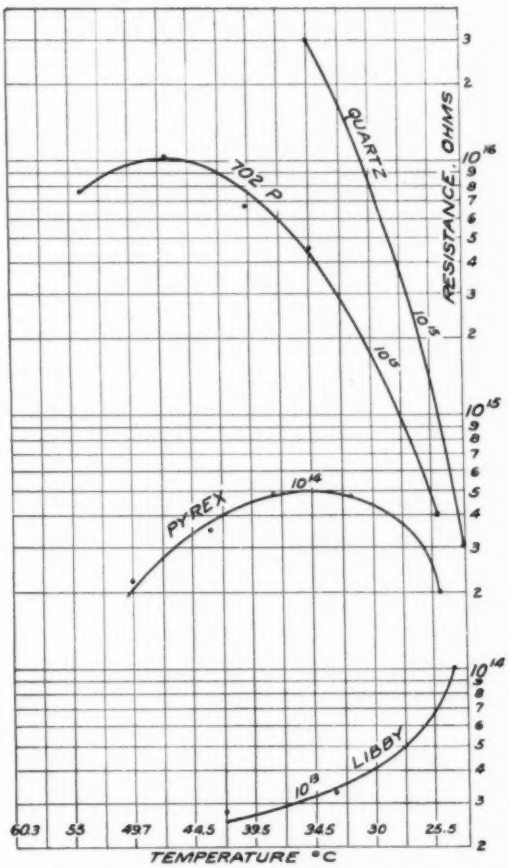

Fig. 9. Variation of resistance with temperature above ambient, on humid summer day.

Dr. L. A. DuBridge, during a succeeding summer, tested the sensitivity of laboratory tubes, and investigated two additional sources of leakage; namely, photoelectric emission from the grid, due, first, to the light of the filament, and second, to soft x-rays produced by impact of electrons on the space charge grid and anode. With a pure tungsten filament, at any practical operating temperature, the photoelectric currents due to the filament light are enormous, of the order of 10^{-12} amperes. A thoriated filament, operating at approximately 1700°K, gives a photoelectric current from a thorium-coated grid of about 10^{-15} amperes.

X-rays from the plate and space charge grid give currents which increase very rapidly with increase of voltage of these elements above the value corresponding to the photoelectric threshold of thorium (2.65 to 3.35 volts, according to thickness of layer). Fig. 10 shows this x-ray photoelectric current as a function of space charge grid voltage. For low voltages of the space charge grid, below 3 volts, the leakage is high because positive ions from the positive end of the filament are able to escape; that is, the grid is not positive enough to perform its function. At high voltages, above 6 volts, the leakage due to x-rays becomes large. The voltage is measured from the negative end of the filament. X-rays from the plate produce similar photocurrents, but of smaller

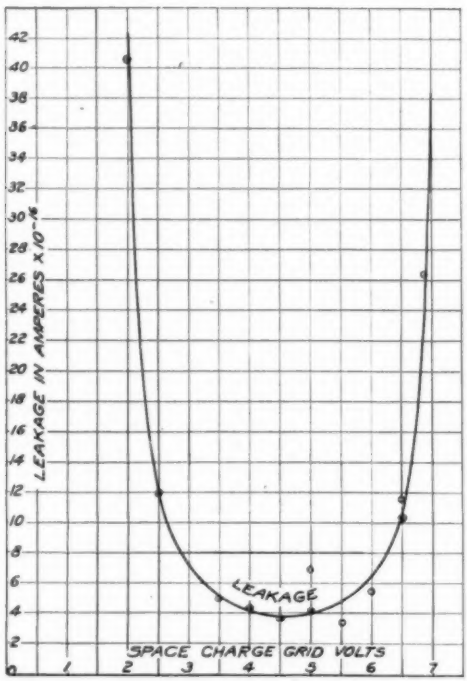

Fig. 10. Photoelectric current from control grid due to x-rays from space-charge grid, as function of voltage of space-charge grid.

magnitude, since the average plate current (40 microamperes) is only a few percent of the space charge grid current.

With these tests as a background, the Vacuum Tube Engineering Department undertook the development of a practical amplifier for small currents, which is known as FP-54 Pliotron.[32] Fig. 11 shows a photograph of this tube, which is of conventional form except for the insulation of the control-grid. A space charge grid maintained at +3 volts with respect to the filament holds back positive ions from the filament. Carefully shielded quartz beads support the grid inside of the tube, quartz being used because glass, at the temperature of these beads, shows volume conductivity. The grid is brought out from

[32] G. F. Metcalf and B. J. Thompson, Phys. Rev. **36**, 1489 (1930).

the top of the tube through clean, low conductivity glass, by a fine wire making minimum contact with the glass. With the plate and space charge grid voltages prescribed by x-rays, and the normal control grid voltage (-3 volts) fixed by the requirement that the grid shall catch no electrons from the filament, the amplification factor is chosen so as to give the desired mutual conductance and plate current. In addition to these structural features, it is necessary to shield the upper part of the tube from both electrostatic fields and ionization of the ambient air, since ions collecting on the wall of the tube

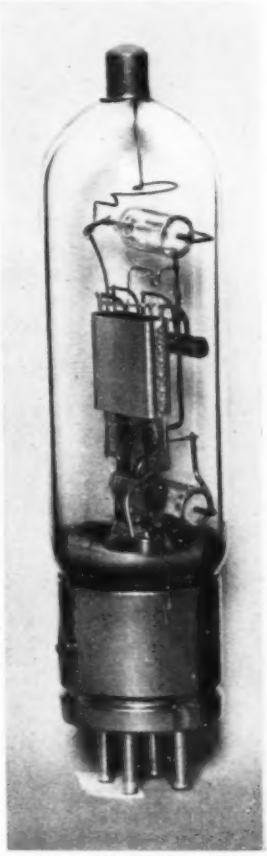

Fig. 11. Photograph of FP-54 Pliotron.

have nearly the same effect as though they condensed on the electrodes inside. Several investigators have shown that vacuum enclosure of the grid lead is worthwhile for maximum sensitivity, on account of radioactive and cosmic ionization in the air.

The circuits used with the FP-54 Pliotron, and the sensitivity obtainable, have been described by Dr. L. A. DuBridge.[33] The circuits are similar to those used by other investigators. With the two tube circuit described by DuBridge, he was as able to measure currents as small as 5×10^{-18} amperes.

[33] L. A. DuBridge, Phys. Rev. **37**, 392 (1931).

This circuit, in order to be balanced, requires a pair of fairly well matched Pliotron tubes. A slight modification of DuBridge's circuit has been devised by T. M. Dickinson, of the Vacuum Tube Engineering Department of the General Electric Company, which does not require matched tubes, and which, in addition, can be made entirely insensitive to small variations of both filament and plate voltages. This circuit is shown in Fig. 12. It is the same as that of DuBridge except for the addition of resistances R_7 and R_8, and of the voltage divider R_1, R_2, R_3, which allows a single battery to furnish plate voltage, space charge grid voltage and control grid bias. The circuit is first adjusted,

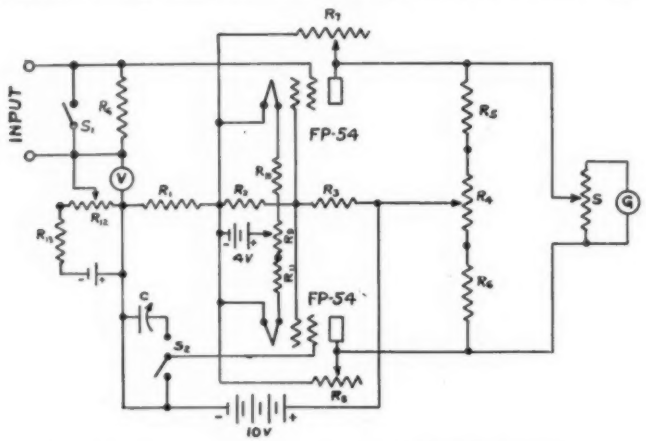

Fig. 12. Two-tube circuit diagram for FP–54 Pliotrons.

$R_1 = 3000$ ohm resistor
$R_2 = 5000$ ohm resistor
$R_3 = 2000$ ohm resistor
$R_4 = 10{,}000$ ohm potentiometer
R_5 and $R_6 = 5000$ ohm resistors
R_7 and $R_8 = 0.1$–10 megohm resistors
$R_9 = 10$ ohm potentiometer
R_{10} and $R_{11} = 15$ ohm resistors
$R_{12} = 400$ ohm potentiometer
$R_{13} = 1000$ ohm resistor
$S = 10{,}000$ ohm potentiometer
$V = 0$–200 MV millivoltmeter
$R_G = 10^{10}$ to 10^{14} ohm resistor
$C = 15 \mu\mu f$ quartz insulated variable condenser
S_1 and S_2 = quartz or air insulated switches
G = sensitive galvanometer

by varying R_9, until no change in the galvanometer reading at balance is caused by small changes in filament voltage. A similar adjustment for plate voltage is then made, by varying either R_7 or R_8.

Recently Dr. L. E. Loveridge, working first at the University of California and later in the Department of Terrestrial Magnetism of the Carnegie Institution at Washington, has obtained an even greater sensitivity with a single tube. The following statement, kindly furnished by Dr. John A. Fleming of the Department of Terrestrial Magnetism, gives the result of Dr. Loveridge's tests to date.

"The Department of Terrestrial Magnetism of the Carnegie Institution of Washington has been interested in determining the ultimate limits of stability of the FP-54 Pliotron when used as an electrometer. Since the sensitivity of the plate-circuit galvanometer can be greatly increased, if desired, over that of the Leeds and Northrup type R galvanometer ordinarily used, the short-period fluctuations and the long-period drifts constitute the real limit to the attainable sensitivity.

"Encouraged by the results obtained with the single-tube circuit by Professor Lawrence and his students (especially L. E. Loveridge) at Berkeley, we set out to determine the limiting fluctuations with the whole tube mounted in vacuo to eliminate fluctuations due to residual ionization. The central system of a Hoffmann duant electrometer is thus protected. Our L. R. Hafstad found that for a tube so mounted, and with its control grid at the 'floating potential', following a suggestion of Professor Ruark, the fluctuations and drifts could be reduced far below any previous value we had attained, provided the batteries (lead cells) were held at constant temperature.

"Further work since September 1931 by Dr. Loveridge, after he became associated with the Department's staff, has shown that the limits obtainable are substantially those found by Mr. L. R. Hafstad, and are about as follows: Using a single FP-54, mounted in air at a pressure below one millimeter, with new lead storage batteries held at constant temperature, with key open (grid floating), the short-time fluctuations (having the galvanometer period of 5 seconds) are less than the deflection corresponding to about 500 electrons on the control-grid, and the steady drift can be held as low as 5000 electrons per hours without serious difficulty (50,000 millimeters per volt, one centimeter drift per hour). The fluctuations are one-half to one-third as large with the key closed (grid bias equals floating potential) as with the key open (grid floating). The exact cause for this is not yet understood. The limits have been found substantially the same for three different tubes, and many changes and tests have been made to eliminate entirely possible fluctuations in the batteries and associated circuits. These short-period fluctuations, as far as we have been able to tell, are inherent in the tubes themselves. The limit of sensitivity for short-time events of unknown time-distribution is thus about 500 electrons, and therefore for events whose time is known, that is, which can be turned on and off, and with a better galvanometer, the limit is perhaps 50 to 100 electrons. For small steady currents, which can be turned on and off, the limit may be one electron per second in a time of several minutes.

"The input impedance with floating grid does not compare badly with that obtainable using resistors and a negative bias. The limitation in use is set by fluctuations rather than impedance in most cases, anyway, especially when it is desired to detect single events, such as single alpha-particles, *H*-particles, or other 'counts'.

"The attached traces are typical of those obtained. The recording rate or time scale is 20 millimeters per minute and sensitivity 500 electrons per milimeter. Curve No. 1 is with key closed and grid bias set at floating potential; curve No. 2 is with key open and grid floating". These traces are shown in Fig. 13.

The limiting sensitivity of small current amplification can be calculated on the basis of shot and *flicker* effect, and thermal agitation. The shot effect fluctuations in the grid circuit of the present FP-54 tube are due to a current of approximately 2×10^{-15} amperes, since the grid current of 10^{-18} amperes is a balance between two nearly equal opposite electron currents of 10^{-15} amperes each. These two currents, one of which is due to the photoelectric effect

of the filament light, and the other, used for balancing, to electrons from the filament (adjustable by grid bias), can probably be reduced by a factor of 10 by removing thorium from the grid. The shot effect in the plate circuit is

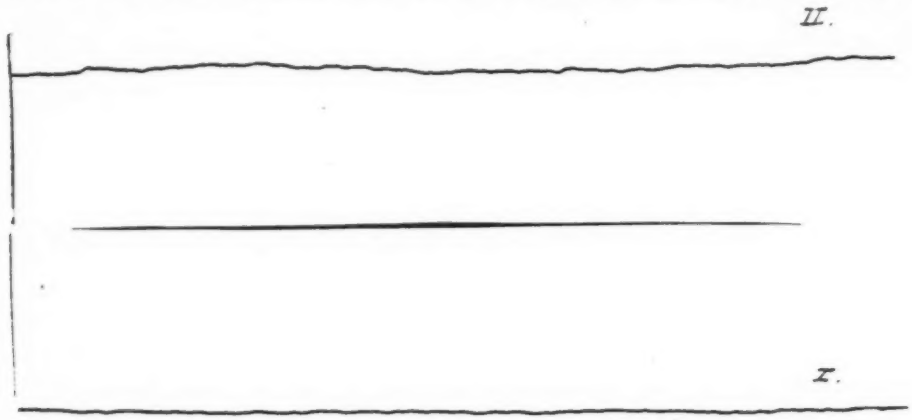

Fig. 13. Recording galvanometer records of FP-54 Pliotron in single tube circuit. Curve I, grid potential fixed by bias battery. Curve II, grid floating. Total length of each record 10 minutes. Maximum deflection in curve I is about 500 electrons; in curve II, about 1000 electrons.

also to be calculated from the total plate current, about 40×10^{-6} amperes, rather than the much smaller net current in the galvanometer circuit.

The amplification of small voltages.—The limitations to the amplification of small alternating voltages are well known.[34] They are due, fundamentally,

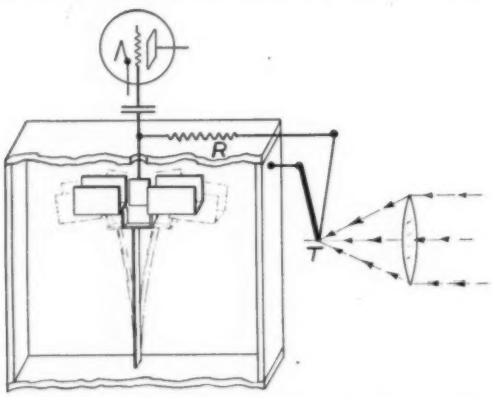

Fig. 14. Arrangement for changing small direct voltage to alternating, by periodic variation of capacity.

to shot effect[35] and to thermal agitation[36] in the input resistance. At low frequencies there may be fluctuations much greater than those due to the normal shot effect,[37] caused by fluctuations in the electron emission of the

[34] A. W. Hull, Phys. Rev. **27,** 439 (1926).

[35] W. Schottky, Ann. d. Physik **56,** 541 (1918); A. W. Hull and N. H. Williams, Phys. Rev. **25,** 147 (1925).

[36] J. B. Johnson, Phys. Rev. **32,** 97 (1928).

[37] J. B. Johnson, Phys. Rev. **26,** 71 (1925).

cathode.[38] Recent experiments[39] show that these fluctuations can be greatly reduced by better evacuation methods, so that the limit of amplifiable smallness may ultimately be the same at low frequency as at high frequency. This limit is approximately 1 microvolt at high frequency, but may be reduced to 1/10 microvolt or less, at low frequency, by restricting the amplifier to a narrow band of frequencies.

The amplification of small *direct* voltage, such as thermal e.m.f., is quite a different matter, and the methods available are too clumsy to merit description. Recently, we have attempted to convert these small direct voltages into alternating voltage. One method, which is described by Mr. G. F. Metcalf in a current issue of this journal, consists in opening an inductive circuit carrying *current*, due to the small e.m.f., by means of a vacuum interrupter. The sharpness of the break produces a high transient voltage, which can be amplified.

Another method, which is yielding promising results, is to vary periodically the input capacity. A typical circuit arrangement is shown in Fig. 14. An insulated electrode is so placed that its capacity to "ground" can be changed periodically by the vibration of a grounded reed. An e.m.f. of a thermocouple T is impressed, through a high resistance R, upon the insulated electrode. If the surface of this electrode is at the same potential as that of the other elements in the "ground" enclosure, no currents will be induced in the circuit by changing the capacity; if at a different potential, current will be induced, and the resulting voltage at the terminals of R can be amplified. Calculation shows that, by making the time of large grid-to-ground capacity long compared to the time during which this capacity is small, a voltage step-up, from d.c. to a.c., may be obtained, of the order of tenfold. Thus it may be possible to measure thermal e.m.f. as low as 10^{-7} volts, produced in a high resistance thermopile.*

The Thyratron

The Thyratron[40] is an arc discharge device whose *starting* can be controlled by a grid. Alternatively, it may be described as a three-element vacuum tube of the Pliotron type containing a small amount of gas. As is well known, the grid is powerless to control the current in a "gassy" Pliotron tube. The reason for this has been fully discussed by Langmuir,[41] and is due to the formation of a very thin "*positive ion sheath*" over the surface of the grid. This sheath contains the whole voltage difference between the grid wire and the space, and insulates the grid from the discharge space as effectively as a layer of varnish. Thus the grid is unable to stop or appreciably modulate the

[38] W. Schottky, Phys. Rev. **28,** 74 (1926).

[39] G. F. Metcalf, Amer. Phys. Soc., Boston meeting, Feb. 25, 1932.

* *Note added May 13, 1932.* An article by Ross Gunn has just appeared (Phys. Rev. **40,** 307 (1932)) describing a similar instrument developed for use in aircraft. The sensitivity (10^{-4} volt) is stated to be "comparable to a Compton electrometer in stable adjustment."

[40] A. W. Hull, Gen. Elec. Rev. **32,** 213, 390 (1929).

[41] I. Langmuir, J. Frank. Inst. **196,** 751 (1923). H. M. Mott-Smith and I. Langmuir, Phys. Rev. **28,** 727 (1926); A. W. Hull and I. Langmuir, Proc. Nat. Acad. Sci. **51,** 218 (1929).

discharge unless the grid wires are so close together, or the sheaths become so thick, that adjacent sheaths touch.

Before the discharge starts, however, when there is no ionization present, the electrostatic conditions are exactly the same as in a high vacuum tube. Hence, if the electric field at the cathode is negative, so as to oppose the escape of electrons, the current can not start. As soon as the grid potential is increased to such a value that a few electrons can escape, of the order of a few microamperes in certain tubes, the resulting ionization rapidly annihilates space charge and the full current allowed by the tube immediately starts. This current is limited only by the circuit resistance, since the voltage drop in

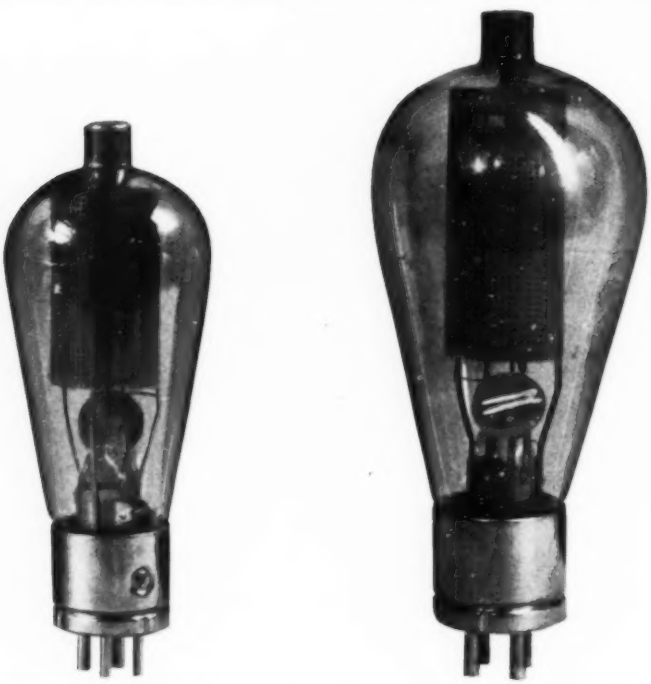

Fig. 15. Small Thyratrons useful for measurement purposes. Left—FG-17. Right—FG-57.

the tube remains constant at approximately the value of the ionizing potential of the gas, for all values of current. The time required for the ionization to build up to the full current value varies from one microsecond to about ten microseconds under different starting conditions.[42] The time required for the ionization to disappear, after the current is interrupted by the removal of the anode supply voltage, is longer, and varies from 10 to 1000 microseconds according to the electrode spacing, gas pressure, and voltage impressed on the electrodes.

The advantages of the Thyratron for measurement purposes are its high

[42] A. W. Hull and L. B. Snoddy, Phys. Rev. **37**, 1691A, 1931. The longer apparent times observed by Nottingham (J. Frank. Inst. 211, 271, 1931) were due to a faulty method of measurement. The other limitations of Thyratrons reported by Nottingham are characteristic of the particular tubes and circuits used, and not inherent.

amplification, low resistance, and the fact that it continues to operate, when once started, until the plate voltage is removed. The amplification is very high compared to the Pliotron. For example, a mutual conductance of 5 m.a. per volt is a large value for a Pliotron. This means that a change of 1 volt in grid potential will produce a change of 5 m.a. in plate current. In a corresponding Thyratron, a change of 1/10 volt will start a current of 5 amperes or even more. The amplification of the Thyratron is thus 10,000 times greater than that of the Pliotron. The power required to start a Thyratron of proper design is the same, or smaller, than that required for the Pliotron, since the only additional grid current in the Thyratron is due to positive ions and constitutes a negative resistance.

Fig. 15 shows two typical small Thyratrons, which are suitable for measurement purposes. They are known as FG-17, a simple filament tube with a rated plate current of $\frac{1}{2}$ ampere and maximum plate voltage of 2500 volts, and FG-57, which is a two ampere Thyratron with equipotential cathode.

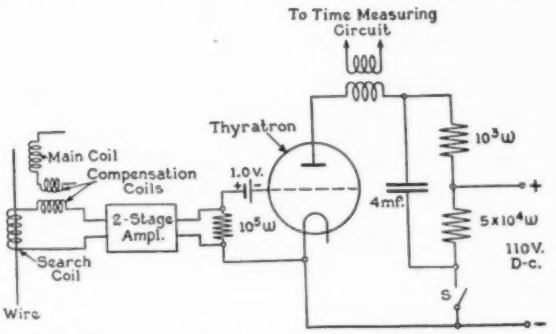

Fig. 16. Thyratron circuit measuring short time intervals.

Both of these Thyratrons have some grid emission at full rated load, which limits the smallness of the input power required to operate them. Such leakage, which is due entirely to thermionic emission from the grid, is easily avoided, and tubes can be provided to furnish any desired current without grid leakage.

A typical application of the Thyratron is shown in a research of Sixtus and Tonks,[43] in which the Thyratron is used to measure short time intervals (Fig. 16). Samuel[44] has described experiments in which a Thyratron is used for obtaining a linear time axis for a cathode-ray oscillograph; and Nottingham[45] for operating thermionic filaments without voltage gradient.

One of the most interesting Thyratron applications is a method of counting alpha-particles devised by C. E. Wynn-Williams.[46] A typical circuit used by Wynn-Williams is shown in Fig. 17, and its operation is described in his own words as follows: "Several Thyratrons, —, —, *P*, *Q*, *R*, *S*, *T*, —, —, —,

[43] K. J. Sixtus and L. Tonks, Phys. Rev. **37**, 930 (1931).
[44] A. L. Samuel, Rev. Sci. Inst. **2**, 532 (1931).
[45] W. B. Nottingham, Phys. Rev. **37**, 1690A (1931).
[46] C. E. Wynn-Williams, Proc. Roy. Soc. **A132**, 295–310 (1931).

are interconnected in such a way that the same voltage impulse is applied simultaneously to *all* their grids; only one Thyratron, however, (suppose Q) can respond (or arc) at a time, the grids of the others being biased too nega-

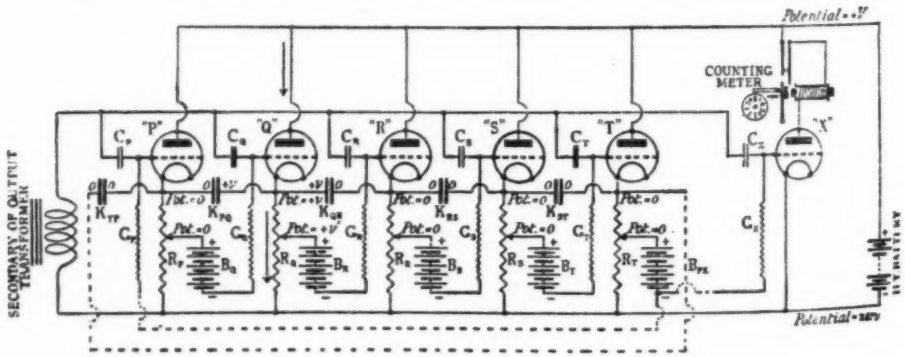

Fig. 17. Thyratron ring for counting alpha-particles (Wynn-Williams).

tively to respond. The arcing of Q immediately 'primes' the next Thyratron in the group (R) *without mechanical aid* so that a second impulse can, if necessary, be registered immediately by R, even before any mechanical counting device associated with Q has commenced to operate. Similarly, subsequent

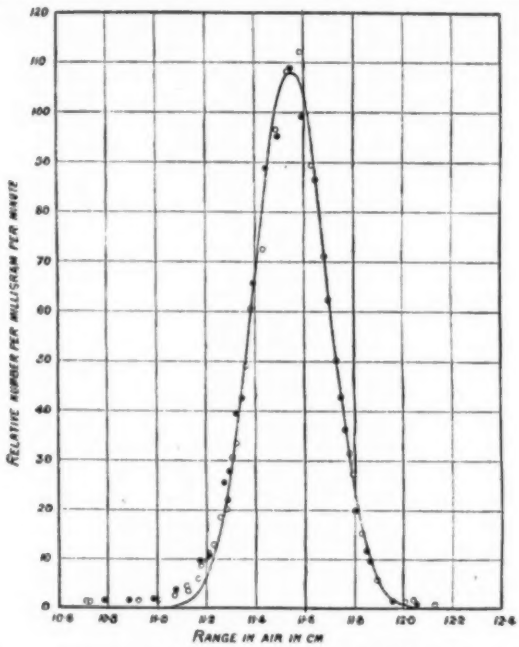

Fig. 18. Two determinations of the range of alpha-particles from Ra C′, using the Thyratron counter. Note repetition accuracy.

impulses are registered by S, T, —, —, and so on. The great advantage of such an arrangement is that the switching can be effected *entirely electrically and independently of mechanical relays*, thus enabling high operating speeds

to be attained. This is done simply by making the arc current of one Thyratron alter the grid bias potential of the next in the group". At the same time, the starting of any Thyratron Q *extinguishes* the preceding one P, by virtue of the condensers K_{PQ}, etc., which link the cathodes together. Thyratron T is coupled to a Thyratron X, whose plate circuit contains a mechanical counter, and it is also coupled to Thyratron P, thus starting the cycle again. "When Thyratron T is operated Thyratron P is primed, and when P is operated, T is extinguished. In this way, successive voltage impulses cause the Thyratrons to arc in the order —, —, P, Q, R, S, T, P, —, —. If, therefore, a counting mechanism be associated with any one Thyratron, say P, every fifth impulse will be recorded. While the meter is still in the process of recording; four more impulses may be recorded by Thyratrons, Q, R, S, T (which need have no meters). There is no need to restrict the number of Thyratrons in the ring to five; any convenient number may be employed greater than two, depending upon the desired maximum counting speed. Rings of three and four Thyratrons have been tried out experimentally, and found to operate in the predicted manner."

Fig. 18, from a paper by Rutherford and Wynn-Williams,[47] shows the accuracy of counting attained with this Thyratron arrangement. The two sets of points, represented by dots and circles respectively, are from two separate experiments using the same source of thorium C′.

As the Thyratron becomes known, it is expected that other scientific uses will be found for it, such as operation of thermostats, voltage regulation, registration of events or actuation of apparatus by means of a beam of light, and the combination of phototube and Thyratron; in short, any operation where an inertialess relay is required.

[47] Rutherford, Wynn-Williams and Lewis, Proc. Roy. Soc. **A133**, 351 (1931).

On the Ultra High-Frequency Oscillation of the Magnetostatic Vacuum Tube

By WALTER DEHLINGER
Westinghouse Electric and Manufacturing Company, East Pittsburgh, Pennsylvania

(Received March 28, 1932)

A physical picture of the phenomena during the electronic oscillation in the magnetostatic oscillator is given. The notion of a critical radius for plate voltages varying between a larger and a smaller value than the critical voltage for a given constant magnetic field is developed. The value of the critical radius is calculated as a function of the voltage differences and the potential distribution. The flying time of the electrons is discussed in its relation to the voltage distribution, and the falling angle is expressed in a simple way.

INTRODUCTION

A "Magnetostatic Oscillator" (abbreviated: MSO) is defined as a generator of electric oscillations using a vacuum tube, having a cathode and one or more anodes, in combination with a constant magnetic field in such a way that the frequency of the oscillation is primarily determined by the anode voltage of the vacuum tube.

The simplest magnetostatic oscillator is substantially composed of a vacuum tube with a cylindrical anode and a hot cathode in the axis of the positive plate cylinder. When a homogeneous magnetic field of a certain *critical*[1,2] value is applied in the direction of the cylinder axis[3,4,5] oscillations are generated in an oscillation circuit between filament and plate.

A variation of the magnetostatic oscillator which yields higher output is obtained by splitting the anode into two semi-cylinders[4] and connecting the two plate halves by an oscillation circuit tuned to a frequency, the period of which is of the order of the critical flying time T_0, i.e., the time it takes the electrons to travel from the filament to the plate under critical conditons.

The purpose of the following investigation is to give a physical picture[6] of the occurrences in the tube during the electronic oscillation.

Parts I and II are devoted to the discussion of the flying time and the falling angle of an electron in a cylindrical magnetostatic oscillator for different potential distributions. In this discussion critical conditions are assumed, and a steady plate current is supposed to flow.

In Part III the conceptions of falling angle and flying time will be generalized for the application during the oscillation. The efficiency of the mag-

[1] A. Hull, Phys. Rev. **18,** 31 (1921).
[2] I. Langmuir and K. T. Compton, Rev. Mod. Phys. **3,** 192 (1931).
[3] A. Slutzkin and D. Steinberg, Ann. d. Physik **1,** 658 (1929).
[4] Okabe and Yagi, Proc. I.R.E. **16,** 715 (1928); Proc. I.R.E. **18,** 1748 (1930).
[5] E. Habann, Jahrbuch d. drahtl. Telegr. **24,** 115, 135 (1924).
[6] H. E. Hollmann, Ann. d. Physik **8,** 956 (1931).

netostatic oscillator will be discussed. In this connection the conception of a critical radius will be developed. This critical radius affects the efficiency of the tube. It is a function of the potential distribution and of the plate voltage amplitude of the oscillation.

I. The Critical Flying Time

The orbits[1] of electrons starting with zero initial velocity from a filament in the axis of a cylindrical anode under the influence of a homogeneous magnetic field in the direction of the cylinder axis are plane curves in planes at right angles to the cylinder axis. The magnetic field deflects the electrons from the radial direction of the electric field and adds an angular component to the force on the electrons.

The critical magnetic field is just sufficiently large to bend the electronic orbits in such a way that they become tangential to the plate. The critical magnetic field is independent of the potential distribution; it depends on the anode voltage only. Therefore the space charge does not influence the critical relation:

$$H_c^2 = \frac{8m}{e} V_c \frac{1}{R^2(1 - r_0^2/R^2)^2} . \tag{1}$$

Here R is the anode radius; r_0 is the filament radius; V_c is the anode voltage.

While the critical magnetic field does not depend on the voltage distribution, the critical flying time T_0 of the electrons from the filament to the plate does:

$$T_0 = \int_{r0}^{R} dr/V_r \tag{2}$$

because the radial velocity V_r depends on the potential distribution. For zero initial velocities, the radial velocity V_r is given by the equation:[1]

$$V_r^2 = \frac{2e}{m} V_r - H^2\left(\frac{e}{2m}\right)^2 r^2\left(1 - \frac{r_0^2}{r^2}\right)^2 . \tag{3}$$

Expressing H in this equation by the voltage V_c from Eq. (1) and replacing V_r—the potential at a distance r from the axis—by $V_c f(r/r_0)$, where V_c is the critical anode potential, Eq. (3) becomes:

$$V_r^2 = \frac{2e}{m} V_c \left\{ f(x) - \frac{(x - 1/x)^2}{(P - 1/P)^2} \right\} = V_m^2 F^2(x) . \tag{4}$$

In (4) x is the ratio r/r_0 and $P = R/r_0$ is the ratio of the radii of anode and filament. The second term in the bracket of (4), is a given function of x. It varies from zero to unity when x varies from 1 to P. The potential distribution $f(x)$ also varies from zero to unity when x varies from 1 to P. Its form varies during the oscillation.

As the flying time depends on the potential distribution, we shall examine the change of flying time with varying potential distribution. The critical flying time T_0 may be defined as the distance from the filament to the plate

divided by the mean radial velocity. This definition will be useful for a qualitative comparison of the values of the flying time corresponding to different potential distributions.

The highest possible mean radial velocity corresponds to *no space charge*, i.e., to a logarithmic potential distribution:

$$f_1(x) = \ln x/\ln P. \tag{5}$$

Neglecting the influence of the magnetic field the space charge function for a cylinder is of the form

$$f_2(x) = (x/P)^{2/3} \tag{6}$$

except in the immediate neighborhood of the filament, where it becomes

$$f_3(x) = \left(\frac{x-1}{P-1}\right)^{4/3}. \tag{7}$$

Of these three potential distributions, the logarithmic distribution f_1 produces the highest average radial velocity; the 4/3 power law f_3 leads to the smallest average radial velocity of the electrons travelling from the filament to the plate. During the oscillation, the electrons will meet potential distributions which are partly steeper, partly flatter than the 2/3 power law. There is an upper and a lower limit of the mean radial velocity connected with the probable steepest and flattest potential distribution actually occurring.

We shall from now on restrict our attention to a ratio P of about 100. For this ratio the space charge field distribution near the filament contributes little to a change of the mean radial velocity. The effect is, however, always a decrease.

There may be local changes of the space charge at other distances from the filament during the oscillation. For an upper limit for the radial mean velocity, we shall assume an average potential distribution half-way in steepness between the 4/3 and the 2/3 power law, say a linear law.

On the other hand the smallest space charge which the electrons will eventually meet during the oscillation is zero. Therefore, the upper limit for the mean radial velocity corresponds to the logarithmic potential.

Let T_m represent the flying time of an electron traveling with uniform radial velocity $v_m = (2eV_c/m)^{1/2}$; then the critical flying time is for the logarithmic and for the linear potential respectively:

$$T_{\ln} = 1.88T_m \tag{8}$$

$$T_1 = 3.12T_m. \tag{9}$$

The critical flying time for a 2/3 power potential distribution is approximately $T_{2/3} = 2.4\ T_m$.

II. The Falling Angle

The electron is deflected from its original radial direction due to the influence of the magnetic field. It arrives, under critical conditions, at the plate

with a purely angular velocity. The angle between the initial radial direction and the radius vector from the filament to the point where the electron reaches the plate defines the falling angle.

The falling angle θ may be calculated from the angular velocity[1]

$$\frac{d\theta}{dt} = H\frac{e}{2m}\left(1 - \frac{r_0^2}{r^2}\right). \tag{10}$$

Integrating (10) for very thin filament the angle θ becomes:

$$\theta = H\frac{e}{2m}\int_0^{T_0} dt = H\frac{e}{2m}T_0. \tag{11}$$

With the same approximation the critical relation between H and V is

$$H_c = \left(\frac{8m}{e}V_c\right)^{1/2}\frac{1}{R}. \tag{12}$$

So the falling angle becomes

$$\theta = \left(\frac{2e}{m}V_c\right)^{1/2}\frac{T_0}{R} = \frac{V_m}{V_r} \tag{13}$$

because $R/T_0 = \bar{V}_r$. Eq. (13) states that the flying angle for an infinitely thin filament is the quotient of the maximum total velocity and the mean radial velocity. From (13) we conclude: The value of the falling angle is roughly 2 and 3 radians respectively for the two limiting potentials considered above. (See Eqs. (8) and (9).)

The exact value of the falling angle depends on the ratio P. In the case of $P = 100$ the angle becomes a little smaller than the ratio given by Eq. (13).

III. Change of Flying Time During the Oscillation Efficiency

A. Period and critical flying time

The magnetic field is kept constant during the oscillation. The plate potential varies above and below the voltage which is in critical relation with the constant magnetic field. In this sense we shall speak of the plate voltage as oscillating above and below the *critical voltage.*

How is the critical flying time connected with the period of the oscillation in the single plate tube?

Infinitesimal plate voltage amplitude.—This case gives an easy approach to our problem because it is not necessary to consider the change of flying time during one half-cycle. As long as the electrons reach the plate their flying time is equal to the critical flying time.

The relation between the period of the magnetostatic oscillator and the flying time of the electrons must fulfill the following condition; the integral of the product of the a.c. components of plate current and plate voltage during the negative half cycle must have a larger absolute value than the integral of the same product during the positive half cycle. (Output must be positive.)

The form of the plate current curve is not known. Therefore, we assume the simplest imaginable shape of the plate current curve, which will fulfill the output condition. This is fulfilled by assuming zero plate current during the positive plate voltage half-cycle and a constant plate current during the negative half-cycle. In order to establish it, the flying time of the electrons leaving the filament at $t=0$ must be exactly $\tau/2$. If this is true, these electrons will arrive at the time the voltage turns negative. (See Fig. 2.)

The instantaneous picture at the end of the positive half-cycle shows the entire space between filament and plate occupied with electrons drawn from the filament during the positive half-cycle $t=0$ to $t=\tau/2$. Before the time $t=\tau/2$ none of these electrons have reached the plate.

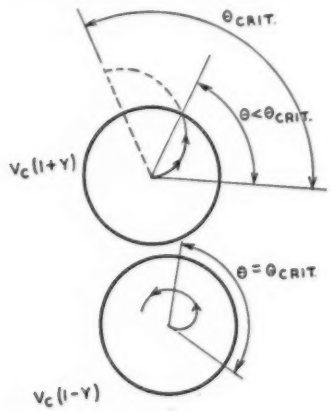

Fig. 1.

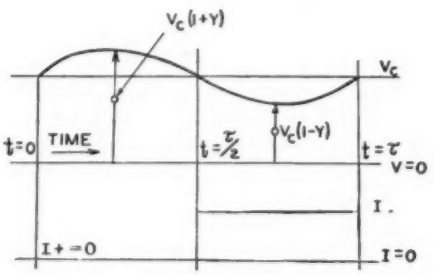

Fig. 2.

We assume that all the electrons under consideration reach the plate during the negative half-cycle. (Later on we shall find that only a large portion of them does; this is, however, not essential for our present aim.)

Now consider the electrons drawn from the filament during the negative half-cycle. At the end of this half-cycle they occupy the space between the filament and a cylinder of a smaller radius than the plate cylinder, because the plate voltage is lower than critical during the half-cycle.

We shall see later, that a part of these electrons will reach the plate during the positive half-cycle. For the relation between flying time and period, it is not necessary to consider this current. For small amplitude our picture suggests the relation:

$$T_0 = \tau/2. \tag{14}$$

Finite plate voltage amplitude.—We assume again that at the end of the positive half-cycle the space between filament and plate is completely occupied by all the electrons which left the filament during the positive half-cycle. The actual flying time of the electrons leaving the filament at $t=0$ must be equal to $\tau/2$. This, however, is shorter than the critical flying time, because the plate voltage was higher than critical during the positive half-cycle. A simple consideration shows that the lower limit of the actual flying time T_a compared with the critical flying time T_0 is given by

$$T_a = \frac{T_0}{(1 + 2/\pi)^{1/2}} = 0.8T_0. \tag{15}$$

In the split plate tube two frequencies can be generated with the same d.c. plate voltage. This means that two kinds of oscillations can be generated with this tube. The first kind of oscillation takes place with about the same frequency as the one observed in a single plate tube of the same anode diameter at the same plate voltage. The relation between the flying time and the period of oscillation is, therefore, the same as in the single plate tube, *viz.*,

$$T_a = \tau/2. \tag{16}$$

Fig. 4 shows the currents arriving at plate half I and plate half II due to the electrons starting under the influence of plate half I. (See Fig. 3.) The

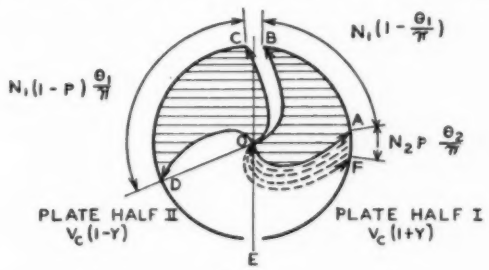

Fig. 3.

voltage curve of plate half I is drawn out; the voltage of the plate half II is dotted in Fig. 4. θ_1 (Fig. 3) is the falling angle for the higher plate voltage, *viz.*, $V_c(1+y)$. This angle is, therefore smaller than the critical falling angle. The letter p represents a true fraction, which shall be explained later.

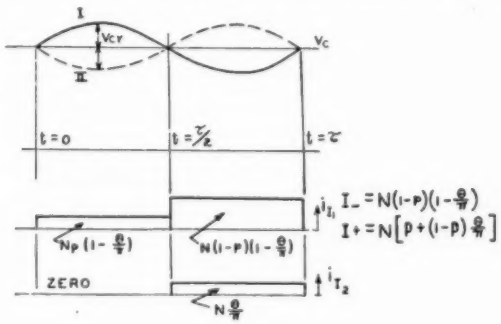

Fig. 4.

The principle of coordinating the flying time T_a to the half period is the same as in the single plate tube. The falling angle is a new factor in this tube, which makes the consideration more complicated, and due to this, the current I_+ arriving at the positive plate half cannot become zero.

The second kind of oscillation which was observed in the split plate tube is characterized by $T_a = \tau/4$. It is very weak and we shall not discuss it here.

Expressing the period in terms of the critical flying time we find the following limits for the longest and shortest value of the natural period:

$$\tau_{\min.} > 1.55T_0 \qquad (17) \qquad\qquad \tau_{\max.} < 2T_0. \qquad (18)$$

For practical purposes, it is more convenient to express the period in terms of the flying time

$$T_m = \frac{R - r_0}{(2c/m)V_c)^{1/2}}$$

of an electron travelling with uniform velocity corresponding to a voltage drop V_c, because this expression contains measurable quantities only. The extreme values for the period are:

$$\tau_{\min.} > 2.88T_m \qquad (19) \qquad\qquad \tau_{\max.} < 6.2\,T_m. \qquad (20)$$

The minimum value of the period refers to logarithmic potential (no space charge) and largest possible plate voltage amplitude; the maximum value refers to linear potential distribution (maximum space charge) and very small plate voltage amplitude.

B. Efficiency and critical radius

The efficiency of the magnetostatic oscillator depends on the ratio of the currents which arrive at the anode (or at the plate halves) during the negative and the positive half cycle of the a.c. plate voltage. As a first step toward an estimate of this ratio for the single plate tube, we consider the following two problems which lead to the notion of the critical radius.

Problem 1.—What condition must be fulfilled in order that electrons starting from the filament under the influence of a plate voltage higher than critical, say $V_c(1+y)$, will arrive at the plate if the plate voltage is suddenly lowered to a value below critical, say $V_c(1-x)$, at a moment when the electrons are on their way from filament to plate?

The answer is that only those electrons will reach the plate which at the time when the plate voltage is lowered are at a distance from the axis larger than a certain radius which can be calculated if the potential distribution is given. This calculation is carried out in the appendix.

With a potential distribution $f(r) = (r/R)^n$ this radius ρ_0 is (see appendix) given by

$$\left(\frac{\rho_0}{R}\right)^n = q^n = \frac{x}{x+y}. \qquad (21)$$

Eq. (21) defines the critical radius ρ_0.

Problem 2.—What condition must be fulfilled in order that electrons leaving the filament under the influence of a plate voltage smaller than critical, say $V_c(1-y)$, will reach the plate if the plate voltage is suddenly raised above its critical value, say to $V_c(1+x)$ while the electrons are under way?

The same critical radius defined by (21) plays a part, but this time the condition for the arrival of the electrons is that their distance from the axis is smaller than the critical radius ρ_0 at the time the plate voltage is changed.

The importance of the critical radius for the phenomena in the *single plate tube* in the case of a rectangular shaped oscillation is evident. Here the

ratio of the amplitude to the d.c. voltage is equal to y, and the value of x in the equation for the critical radius is equal to y. Therefore, we have according to (21)

$$q^n = \left(\frac{\rho_0}{R}\right)^n = \frac{y}{y+y} = \tfrac{1}{2}. \tag{22}$$

The numerical value of $q = \rho_0/R$ depends on the potential distribution, which determines the value of the exponent n. For $n = 1$, the value of q is 0.5; further q becomes smaller with decreasing n; $n = 2/3$ gives $q = 0.354$. For the logarithmic potential $q = 0.165$.

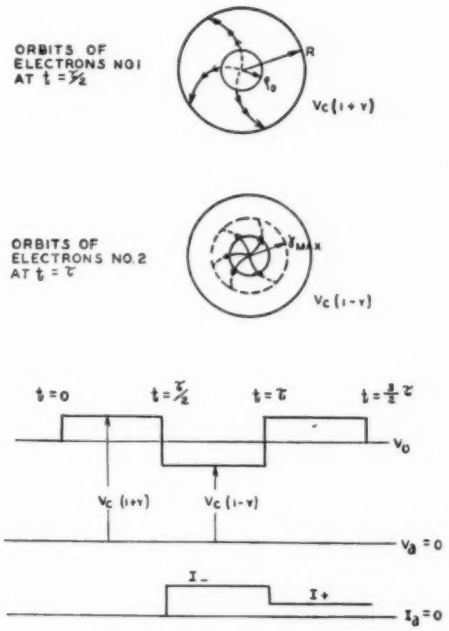

Fig. 5.

During a sinusoidal plate voltage oscillation, the value of the critical radius will vary with the time. This will complicate the phenomena during the oscillation. In order to simplify the description, the phenomena during a rectangular shaped plate voltage oscillation will be described. This kind of oscillation will take place as follows: (See Fig. 5.) The electrons No. 1 leaving the filament during the positive half-cycle (from $t = 0$ to $t = \tau/2$) will just occupy the entire space between the filament and the plate at the time $t = \tau/2$. Not all of these electrons will arrive at the plate during the negative half-cycle (from $t = \tau/2$ to $t = \tau$), but only those that are contained in a cylindrical ring for which $\rho_0 \leqq r \leqq R$. These latter electrons form the plate current I_-.

The electrons No. 2 leaving the filament during the negative half-cycle (from $t = \tau/2$ to $t = \tau$) occupy at the time $t = \tau$ the space between the filament and a cylinder of radius $r_{max} < R$. The value of r_{max} may be greater or less than ρ_0, depending on the plate voltage amplitude. r_{max} will be nearly equal

to R for small amplitude, but for larger amplitude it may even become smaller than ρ_0. Therefore, all the electrons No. 2 will reach the plate for large amplitude. For very small amplitude only a part of the electrons No. 2 will reach the plate. The electrons No. 2 arriving at the plate make up the plate current I_+. The current during one half-cycle is certainly not constant. Since we do not know its law of variation we assume it to be constant. The average current so assumed is equal to $2/\tau \int_0^{\tau/2} i dt$, which we denote by I_+ and I_- for the positive and negative half-cycle respectively.

If we choose $\tau/2$ as the unit of time, we have the advantage that the values of I_- and I_+, are numerically equal to the number of electrons arriving at the plate during each half-cycle.

For the rectangular shaped oscillation so defined, the efficiency reduces to the simple form

$$y \frac{I_- - I_+}{I_- + I_+}.$$

The phenomena in the *split plate tube* are much more complicated, because the effect of the slots between the plate halves cannot be expressed in a simple way. In addition the falling angle must be introduced as a function of the time. The critical radius also changes with the time in a complicated way. In order to approach these phenomena, we return to Figs. 3 and 4. Fig. 3 represents the flow of electrons in a split plate tube for steady plate voltage, *viz.*, $V_c(1+y)$ at plate half I and $V_c(1-y)$ at plate half II. Let the electric field in each plate half be strictly cylindrical, i.e., neglect the distortion of the electric field due to the influence of one plate half on the other.

Then the electrons No. 1 leaving the filament under the influence of plate half I arrive partly at plate half I; partly at plate half II. Let the falling angle corresponding to $V_c(1+y)$ be θ_1. That part of the electrons No. 1 which arrives at plate half I will, therefore, strike this plate half between A and B, where the angle $AOB = \pi - \theta_1$. Let the number of electrons No. 1 escaping from the filament under the influence of plate half I be N_1. The number of the electrons No. 1 which arrive between A and B is, therefore, $N_1(1-\theta_1/\pi)$, if we neglect the electrons escaping through the slot.

The rest of the N_1 electrons No. 1 enters the region which is under the influence of plate half II. Their number is $N_1\theta_1/\pi$. These electrons started from the filament under the voltage $V_c(1+y)$. Now they suddenly come under the influence of $V_c(1-y)$. Therefore, not all of them arrive at plate half II. Only a fraction of them will, namely those whose distance from the filament was larger than ρ_0. Let $(1-p)$ be this fraction. The number of electrons No. 1 arriving at plate half II is therefore $(1-p)N_1\theta_1/\pi$.

A similar consideration on the N_2 electrons No. 2 starting from the filament under the influence of plate half II shows, that none of them arrive at plate half II, but a fraction of them arives at plate half I; the number of these electrons is

$$pN_2(\Theta_0/\pi)$$

where θ_0 and N_2 are falling angle for critical conditions and number of the electrons No. 2. In Fig. 4 these relations are applied to the varying plate

potentials during the oscillation. Due to the finite velocity of the electrons, the voltage of the two plate halves changes during the time the electrons are on their way from the filament to the plate halves.

In Fig. 4, the currents i_1 and i_2 arriving at the respective plate halves are expressed by the number of electrons arriving during the half period as unit time, as before. I_- and I_+ are the plate currents arriving during the negative and the positive half cycles respectively.

Only half of the currents arriving at the plate halves is indicated in Fig. 4, *viz.*, that half which is due to electrons No. 1 drawn from the filament under the influence of plate half I. This does not change the ratio I_-/I_+ it merely avoids a more complicated representation. In Fig. 4, the simplification $N_1 = N_2$ and $\theta_1 = \theta_0$ has been introduced, which is satisfactory for small voltage amplitudes.

For this case we find as the condition for positive output (see Fig. 4)

$$1 - 2p - 2(1 - p)\Theta/\pi > 0. \tag{23}$$

The numerical estimate of the efficiency and a generalization of the picture of the phenomena in the MSO is subject to further investigation.

Appendix

Critical radius for varying plate potential

The equation[1] for the radial velocity of an electron starting at a distance r_0 from the axis of a cylindrical anode under the influence of an axial magnetic field H with the initial velocity components u_0, v_0 is:

$$\left(\frac{dr}{dt}\right)^2 = \frac{2e}{m}V_{rr_0} - H^2\left(\frac{e}{2m}\right)^2 r^2\left(1 - \frac{r_0^2}{r^2}\right)^2 - H\frac{e}{m}r_0 v_0\left(1 - \frac{r_0^2}{r^2}\right) + v_0^2\left(1 - \frac{r_0^2}{r^2}\right) + u_0^2. \tag{1}$$

Here V_{rr_0} is the voltage difference between $r = r$ and $r = r_0$ which can be calculated if the voltage distribution is known. u_0 is the initial radial velocity. v_0 is the initial velocity in angular direction $r_0(d\theta/dt)_{r=r_0}$.

In the first problem stated in paragraph III, the magnetic field is constant; the plate voltage is first higher, later lower than the voltage which is in critical relation to the magnetic field.

Call the plate voltages $V_c(1+y)$ and $V_c(1-x)$ before and after the change respectively.

First calculate the velocity components of an electron at $r = \rho$, which started from an infinitely thin filament with zero initial velocity under the influence of a magnetic field $H_c = (8mV_c/e)^{1/2}$ and a plate voltage $V_c(1+y)$. (2)

From Eq. (1) we find

$$\left(\frac{dr}{dt}\right)^2_{r=\rho} = \frac{2e}{m}\left[V_c(1 + y)\right]_\rho - \frac{2e}{m}V_c\frac{\rho^2}{R^2} \tag{3}$$

where[1]

$$\left(\frac{2e}{m}V_c\right)^{1/2}\frac{\rho}{R} = \rho\left(\frac{d\theta}{dt}\right). \tag{4}$$

These values of $(dr/dt)_\rho$ and $\rho(d\theta/dt)_s$ are now introduced into Eq. (1) as initial velocities u_0, v_0 of an electron starting at $r_0=\rho$ under the influence of a plate voltage $V_c(1-x)$.

Eq. (1) becomes

$$\left(\frac{dr}{dt}\right)^2_{r>\rho} = \frac{2e}{m}[V_c(1-x)]_{r\rho} - \frac{2e}{m}V_c\frac{r^2}{R^2}\left(1-\frac{\rho^2}{r^2}\right)^2 - \frac{4e}{m}V_c\frac{\rho^2}{R^2}\left(1-\frac{\rho^2}{r^2}\right) + \frac{2e}{m}V_c\frac{\rho^2}{R^2}\left(1-\frac{\rho^2}{r^2}\right) + \frac{2e}{m}[V_c(1+y)]_\rho - \frac{2e}{m}V_c\frac{\rho^2}{R^2}. \tag{5}$$

At the plate, for $r=R$, the radial velocity is given by

$$\left(\frac{dr}{dt}\right)^2_R = \frac{2e}{m}[V_c(1-x)]_{R\rho} - \frac{2e}{m}V_c\left(1-\frac{\rho^2}{R^2}\right)^2 - \frac{4e}{m}V_c\frac{\rho^2}{R^2}\left(1-\frac{\rho^2}{R^2}\right) + \frac{2e}{m}\frac{\rho^2}{R^2}V_c\left(1-\frac{\rho^2}{R^2}\right) + \frac{2e}{m}[V_c(1+y)]_\rho - \frac{2e}{m}V_c\frac{\rho^2}{R^2}. \tag{6}$$

The electron will arrive at the plate, when

$$(dr/dt)_R \geqq 0. \tag{7}$$

All the terms on righthand side of Eq. (6) cancel, except

$$\frac{2e}{m}[V_c(1-x)]_{R\rho} - \frac{2}{m}V_c + \frac{2e}{m}[V_c(1+y)]_\rho$$

and Uneq. (7) becomes:

$$(1-x)_{R\rho} - 1 + (1+y)_\rho \geqq 0. \tag{8}$$

Eq. (8) is the condition, that an electron arrives at the plate, which started from the filament under the influence of a plate voltage $V_c(1+y)$, and this plate voltage was suddenly changed to $V_c(1-x)$ when the electron was at a distance ρ from the axis.

Similarly the condition, that an electron arrives at the plate, which started from the filament under the influence of a plate voltage $V_c(1-y)$, and this plate voltage was suddenly changed to $V(1+x)$ when the electron was at a distance from the axis, is

$$(1+x)_{R\rho} - 1 + (1-y)_\rho \geqq 0. \tag{9}$$

Assuming a voltage distribution

$$V_r = V_a(r/R)^n. \tag{10}$$

Eqs. (8) and (9) become

$$\left(\frac{\rho}{R}\right)^n \geqq \frac{x}{x+y} \tag{8'}$$

$$\left(\frac{\rho}{R}\right)^n \leqq \frac{x}{x+y}. \tag{9'}$$

From this follows the definition of the critical radius ρ_0:

$$\left(\frac{\rho_0}{R}\right)^n = \frac{x}{x+y}. \tag{11}$$

Experimental Study of Parallel-Cut Piezoelectric Quartz Plates

By GERALD W. FOX AND W. G. HUTTON
Physics Laboratory, Iowa State College

(Received April 18, 1932)

Y-cut piezoelectric quartz plates were studied with respect to the charges developed on the plates when oscillating near their resonant frequencies. The attractive force between crystal and electrodes was measured. Two methods for determining the piezoelectric voltage developed across the crystal are suggested. It is concluded from a study of crystal breakage that fracture is due to intense mechanical vibration.

ALTHOUGH a large power output is not necessary in using a crystal-controlled vacuum tube for frequency-stabilization purposes, it is of interest to find out what voltage high-frequency quartz plates will stand before they fracture and to form some idea of the cause of shattering. To carry out this investigation, fifteen plates were cut from a large specimen of Brazilian quartz of optical quality. The plates were all of the so-called thin or

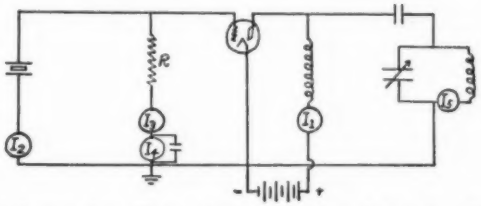

Fig. 1. Standard crystal oscillator circuit—used to determine V_c by method 1.

Y-cut, having their faces parallel to both an electric and the optic axes. Their frequencies were in the range from 3500 to 4000 k.c. This range was chosen because it has been shown[1] that plates whose thickness is represented

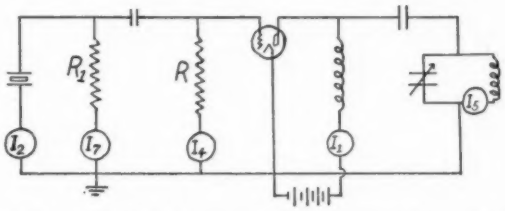

Fig. 2. Modified circuit used to determine V_c by method 2.

by frequencies of this order, provide the largest energy feed-back through the plate to grid capacity and thereby develop an especially large piezoelectric voltage across the crystal, and because plates in this frequency range represent a thickness of material which is still quite strong mechanically.

The standard crystal oscillator circuit (Fig. 1) was used, in which the crystal was connected between the grid and the filament of a three-electrode

[1] Crossley, Proc. I.R.E. **15**, 9–36 (1927).

vacuum tube. A slight modification was made (Fig. 2) in order to have two methods for determining the piezoelectric voltage developed across the crystal. Tubes of the type UX-210 and UV-211 were used in different parts of the work.

Attraction between the Electrodes and the Crystal

In some preliminary experiments, the decided force of attraction between the crystal and the electrodes appeared sufficiently interesting to warrant more careful examination. Accordingly, the lower electrode was made of a heavy plane brass plate while the upper electrode consisted of a light brass disk of about the same size as the crystal. This electrode was connected, by means of an insulating silk thread, to a previously calibrated Jolly balance. A very fine wire of negligible weight made the necessary electrical connection from this plate. Results indicated that the attraction between the upper electrode and the crystal, when plotted against a varied high-frequency current in the tank circuit, changed nearly linearly to a maximum value and then decreased; the maximum attraction occurring before maximum tank current was reached, a result which indicates that the feed back voltage was actually smaller at resonance than before it. A typical set of data shows that with a spring constant of 200 mg/cm the maximum force necessary to pull the upper electrode free from the crystal varied from approximately 0.1 gram at a plate voltage of 150 volts to nearly 10 grams at 300 volts. This represents a hundred-fold increase in charge developed for only a two-fold increase in plate voltage. If the upper electrode and the upper surface of the crystal are considered as a parallel plate condenser, it is possible to obtain an estimate of the surface density of charge. It is $\sigma = V_c/4\pi d$ where V_c is the piezoelectric voltage across the crystal and d is the distance between the plate and the electrode. If we assume that d is 0.1 mm and V_c (from the later work) is of the order of 100 volts for plate voltages as used practically, σ is found to be 2.6 e.s.u./cm^2. The force of attraction when near resonance is very pronounced showing that the surface charge is many times that which could be produced by static compression. Calculation shows that to produce the same charge by simple compression would require a pressure of nearly 10^9 dynes/cm^2 which is equivalent to 1.2 tons and would, obviously, crush the crystal. These values are in agreement with Van Dyke,[2] who says that to develop a piezoelectric voltage of 100 volts across the crystal, a steady applied force of 1 ton/cm^2 would be necessary.

Study of Crystal Breakage

To prevent sparking between the crystal and electrodes when high plate voltages were used, each crystal, when under test, was placed between electrodes in a highly exhausted glass cell. The plate voltage on the vacuum tube was then increased by steps while the plate tank circuit was kept tuned to resonance with the crystal. For each increase in plate voltage, observations were made of the currents in the different branches of the circuit. This was

[2] Van Dyke, Proc. I.R.E. **16**, 742–764 (1928).

continued until the quartz plate shattered or until the limiting voltage (1500 volts) was reached.

Two indirect methods were used to calculate the voltage developed across the crystal (V_c) since there appeared no way of measuring it directly. The use of a vacuum tube voltmeter or even of an electrometer of very small capacity proved out of the question, since the extra capacity of the measuring instrument in parallel with the crystal, provided a shunt capacity which divided the feed-back to such an extent that the crystal would stop vibrating or at best would vibrate very weakly.

In the first method, the circuit shown in Fig. 1 was used. If R is a pure resistance of known value, V_c can be computed from I_3 and I_4. I_3 is the d.c.+a.c. through R as measured by a thermocouple and I_4 is the d.c. through R. Let e be the instantaneous value of V_c and i the instantaneous value of I_3. By definition:

$$I_4 = \frac{1}{T}\int_0^T i dt$$

$$I_3 = \left(\frac{1}{T}\int_0^T i^2 dt\right)^{1/2}$$

where T is the period of the e.m.f. Now, since the e.m.f. is periodic, it is of the form:

$$e = e_4 + \sum_{n=1}^{\infty} e_n \sin(n\omega t) + \sum_{n=1}^{\infty} \epsilon_n \cos(n\omega t)$$

where e_4 is the instantaneous d.c. voltage across R. Carrying through the analysis, the results are that

$$e_4 = I_4 R \tag{1}$$

and

$$e^2 = R^2 I_3^2 = e_4 + (1/2)\sum_{n=1}^{\infty} e_n^2 + (1/2)\sum_{n=1}^{\infty} \epsilon_n^2. \tag{2}$$

It is clear that all of the following e_1, e_2, e_3, etc. and ϵ_1, ϵ_2, ϵ_3, etc. which appear in the equation cannot be found. However, if the e.m.f. is of the form

$$e = e_4 - e_0 \sin(\omega t) \tag{3}$$

the result is

$$e = R^2 I_3^2 = e_4^2 - (1/2)e_0^2 \tag{4}$$

where e_0 is the peak voltage of the a.c. across R. This gives the value

$$e_0 = R(2I_3^2 - 2I_4^2)^{1/2}$$

and the effective value is

$$V_c = e_0/2 = R(I_3^2 - I_4^2)^{1/2}.$$

It seems likely that e would be of the form (3), since the crystal has such good frequency regulation and the circuit a low decrement.

In method 2, a small condenser was placed between the crystal and grid leak R. Another resistance R_1 was used to shunt the crystal. The current (I_7) through R_1 was purely a.c. and measured by a thermocouple. R_1 was a pure resistance of known value so that V_c was computed directly as $V_c = R_1 I_7$.

In Table I are two sets of results for comparable values of plate voltage. One should expect the voltage developed across the crystal to be less by the second method, since here we are shunting the crystal by an extra resistance.

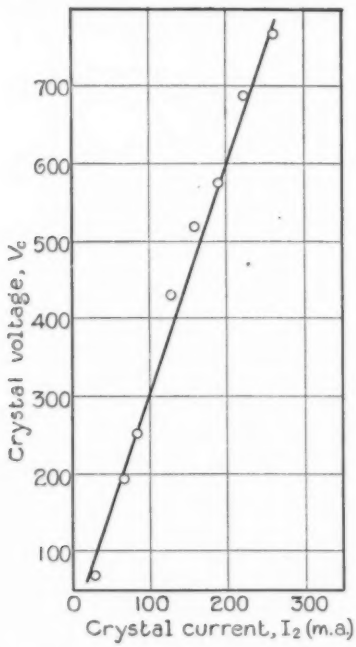

Fig. 3. Graph showing linear relation between crystal current (m.a.) and crystal voltage.

TABLE I. *Calculated values of crystal voltage by methods 1 and 2.*

Method 1		Method 2	
V_b	V_c(calc.)	V_b	V_c(calc.)
100	66	100	44
150	116	150	108
200	159	200	144
250	204	250	186
300	281	300	266
350	310	350	295
400	371	400	368

It was found that the relation between the crystal voltage V_c and the crystal current I_2 was linear. Both increased in value until the crystal either broke or stopped vibrating for some other reason. Data were obtained to show this relation to quite surprisingly large values of V_c. A graph representing a typical case is shown in Fig. 3.

Fig. 4 shows a circular crystal which cracked near the center, a break typical of this shape. Fig. 5 shows a break typical of a rectangular crystal.

DISCUSSION

A study of the broken crystals showed that the fractures always occurred near or in discolored spots. These spots were caused by sparking when the crystal was used in air. Since electrical breakdowns take place between points

of highest potential, the spots were assumed to be the most piezoelectrically responsive parts of the crystals. In the vacuum chamber, there was no sparking. These facts seem to indicate that breaking is not due to heating but more likely to intense mechanical vibration. In every case, the rectangular plates chipped on an edge or corner. If shattering is due to intense mechanical vibration, this would indicate that rectangular plates vibrate most strongly at their extremities. It may be that at high voltages, the simple type of vibrations, the *Y*-cut plates are supposed to execute, become more complex. Unfortunately, no study by dust figures was made. The circular plates always fractured near the center, leading one to believe the amplitude of oscillations was greatest there.

Fig. 4. Typical fracture for round plate.

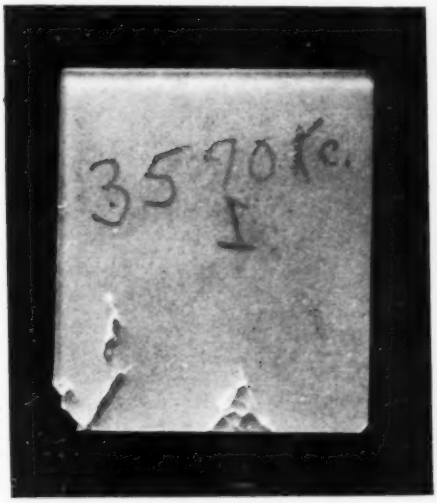

Fig. 5. Characteristic fracture for rectangular plate.

It should be added that a good piezoelectric quartz plate is difficult to break. Some of the plates would stand all the voltage that could be applied to a UX-210 tube without overloading some other elements of the circuit. The plate voltage was increased to as high as 1400 or 1500 volts in the cases of some of the round plates without breaking them. On the other hand, experience shows that poor vibrators break easily. Some were broken at plate voltages of 200 to 300 volts. Poor vibrators are unsteady, that is, they go in and out of vibration, and thus suffer sudden strains which at higher plate voltage may exceed the elastic limit.

The investigation leads one to believe that circular plates are to be preferred. They are, on the whole, more uniform in response and will stand larger loads. The fact that all the plates used were cut from the same piece of quartz and received as nearly identical treatment as possible but that some turned out excellent vibrators while others were poor, seems to indicate variation in the structure of the raw material throughout its mass. The fact that poor vibrators break easily is evidence for a weaker crystalline structure in the strain areas, permitting smaller stresses to produce fractures.

An Electrostatic Alternator

By CHARLES A. CULVER
Carleton College

(Received April 18, 1932)

In electrical measurements and research work it is frequently necessary to have available a source of e.m.f. having a sine wave form. It is also desirable to be able to produce electrical wave forms having special contours. Existing means for producing special e.m.f. wave forms have serious limitations. By utilizing a continuously varying capacitance, means are developed whereby a pure sine wave, as well as special forms, may be produced. Filtering is not required. The theory underlying the production of any desired wave form is outlined. Factors which tend to modify the resultant wave form are pointed out.

INTRODUCTION

THE desirability of having available for use in electrical measurements and for other purposes a source of e.m.f. whose wave form is a sine curve is well known. It is also sometimes useful and convenient in research and development work to have at one's disposal an electrical wave having a special form.

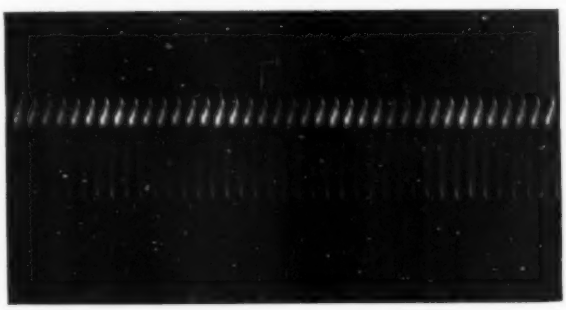

Fig. 1. e.m.f. wave form given by microphone hummer.

Various devices and agencies have been developed for the purpose of producing an e.m.f. having a sine curve form. One of the earliest devices of this character is the Vreeland Sine Oscillator. This piece of equipment yields a pure sine wave form within fairly wide limits of frequency. The first cost of the Vreeland oscillator is however relatively great.

Another, and comparatively simple, organization which is frequently utilized as a source of alternating current for measurement purposes is the microphone hummer; its wave form is not a pure sine function and is not symmetrical with respect to the zero axis; further the amplitude of the wave varies with the load. The first two limitations are evident from the oscillogram shown as Fig. 1.

The thermionic tube will of course produce alternating currents between

extremely wide frequency limits. The wave form, however, is in general not simple, though by the use of filters it can be "purified." Filtering necessitates special capacitances and inductances which are not always available in a given research or testing laboratory

It was for the purpose of making available an alternating current generator which would yield, by relatively simple means, a sine or other desired wave form that the generator about to be described was developed.

THEORY

The theory involved in the new alternator is essentially the same as that which is involved in the condenser transmitter as originally developed by Wente.[1]

In the condenser transmitter the capacitance is caused to vary harmonically due to incident sound waves. The varying charging current causes an

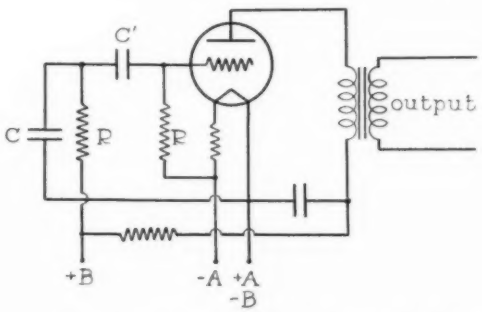

Fig. 2. Amplifier circuit used with condenser transmitter, and as first stage in this investigation.

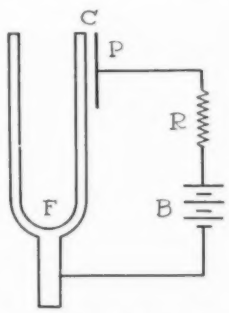

Fig. 3. Tuning fork alternator.

alternating drop across a high resistance; this changing drop is applied between the control grid and the filament of a thermionic amplifier. One of the circuits commonly employed in practice is set forth in Fig. 2. In this diagram C represents the variable capacitance, B the polarizing source of e.m.f. and R the resistance through which the charging current passes. The functions of the other components of the circuit are obvious.

In the case of the condenser transmitter we are dealing with a unit of the parallel plate type, the capacitance of which is given by the relation

$$C = KA/4\pi d \tag{1}$$

where A is the effective area and d the distance separating the plates. Impinging sound waves cause harmonic variations in d. It may be shown[1] that the current through the circuit B-R-C is given by the expression

$$i = \frac{EC}{C_0[(I/C_0\omega)^2 + R^2]^{1/2}} \sin(\omega t + \phi) \tag{2}$$

[1] E. C. Wente, Phys. Rev. **10**, 39–63 (1917).

where C is the maximum capacitance, C_0 the residual or quiescent capacitance of the condenser used as a transmitter, and E the e.m.f. of the source B.

Since the p.d. applied between the grid and filament of the amplifying tube will at any instant be given by $e = Ri$, it follows that

$$e = \frac{ECR}{C_0\left[(1/C_0\omega)^2 + R^2\right]^{1/2}} \sin(\omega t + \phi). \tag{3}$$

It thus follows that the output of the amplifying system will, in a case such as the condenser transmitter, be a sine function. Any procedure, then, by which the capacitance may be made to vary as a sine function will therefore give rise to a sine wave e.m.f. in the output circuit of the amplifier.

Tuning Fork Alternator

One simple and effective method of producing this result is to assemble a variable condenser consisting of a well-made tuning fork, F and a fixed plate, P, as shown diagrammatically in Fig. 3. The lettering in Fig. 3 corresponds to that in Fig. 2. If the fork F is caused to vibrate at its own frequency the capacitance of the condenser, formed by one prong of the fork and the plate, will vary sinusoidally, and the output of the amplifying system will be an e.m.f. having a corresponding form. Fig. 4 shows an oscillogram

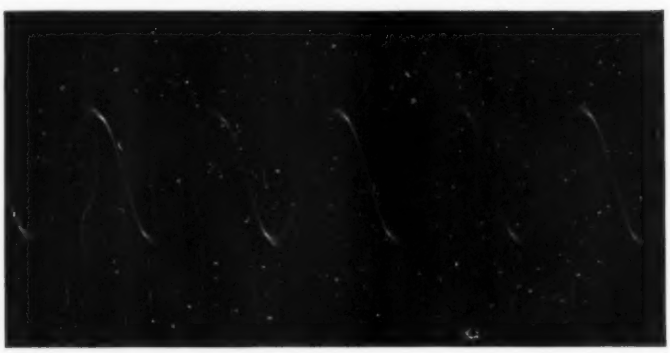

Fig. 4. e.m.f. wave form given by tuning fork alternator.

of the output of such an organization, the frequency in this particular case being 250 cycles. In producing this record the fork was exited by being struck by a soft hammer. It will be noted that the e.m.f. is a pure sine wave and is secured without filtering. By suitable amplification the magnitude of the e.m.f. may be given any desired value. Such an organization may be utilized to develop an alternating e.m.f. for use in many electrical and electrochemical measurements.

One limitation of the method just outlined is that precautions must be observed in order that the tuning fork shall vibrate only at its natural frequency. A second restriction is that the organization will develop only one wave form.

Rotating Electrostatic Alternator

Another electrostatic method of developing an alternating e.m.f., but making use of a somewhat different mechanical arrangement, has been developed. With this second organization various wave forms may be produced. Again referring to Eq. (1), it is apparent that, in the case of a parallel plate condenser, the capacitance is a linear function of the effective area. If, then, the area be caused to vary periodically according to some definite law the capacitance will vary in a corresponding manner.

In order to bring this about one, or a series, of definitely shaped conducting areas may be fastened to an insulating cylinder which is caused to rotate in juxtaposition to a fixed metallic plate, also of definite shape; thus a narrow rectangular area, for example, may be caused to sweep across a second electrode whose contour is of such a form as to give the desired variation in area, and hence in capacitance.

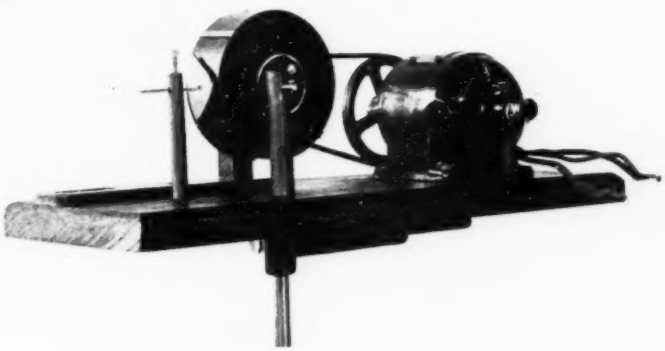

Fig. 5. Rotating electrostatic alternator.

Fig. 5 is a photograph of the preliminary working model with which the results given in this paper were secured. The rotor drum is 9 cm in diameter and made of high grade insulating material. On the outer surface of the rotor and 180 mechanical degrees apart are fastened two rectangular brass electrodes, 3.2 by 0.5 cm. These electrodes are connected to the charging battery *B* by means of a graphite brush bearing on a slip-ring. Since it was desired to study the e.m.f. curves in some detail only two moving electrodes were employed; the individual waves were thus clearly separated from one another on the oscillograph record. The fixed electrode is supported on an insulating pillar. In the photograph (Fig. 5) one of the rectangular electrodes is shown just above the fixed electrode. A small d.c. motor operated from a storage battery drove the rotor at an angular speed of 3600 r.p.m. thus giving a frequency of 120 cycles/sec.

Among the various capacitance areas studied the three shown in Fig. 6 may be mentioned by way of illustration. The triangular area *a* measured 4.2 by 1.1 cm and the electrode designated *b* was 4.5 by 2.5 cm. Area *c* was an unsymmetrical electrode to which reference will be made later.

The polarizing p.d. applied to the generator electrodes was 165 volts. The amplifier employed consisted of three stages, the first two of which were transformer coupled and the last impedance coupled, the final stage containing a 171-A tube. Careful tests have shown that the amplifying system is free from distortion at the frequency employed in these tests.

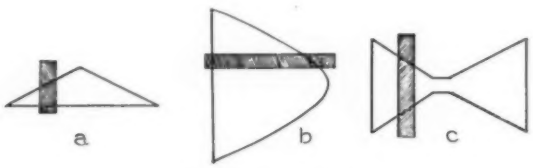

Fig. 6. Typical electrode systems.

In order to illustrate the method of computing the variation in capacitance as the moving electrode sweeps across the fixed area, we may examine the case of the triangular electrode shown as *a* in Fig. 6.

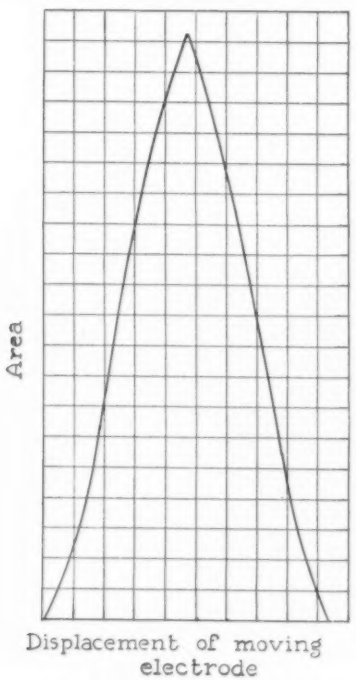

Fig. 7. Area as a function of relative displacement of electrodes shown as *a*, Fig. 6.

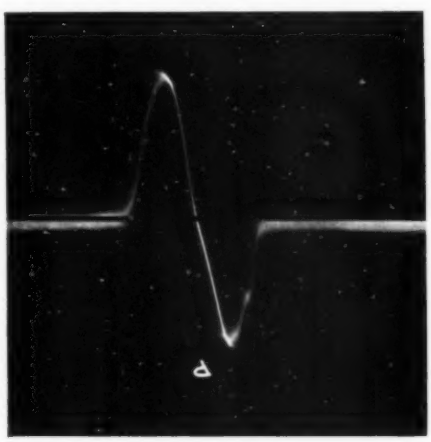

Fig. 8. e.m.f. wave form given by electrode system *a*, Fig. 6.

In this particular case the equation of the bounding curve was

$$x = 2y.$$

The elemental area would be

$$da = ydx.$$

Substitution gives

$$da = (1/2)xdx.$$

Integrating,

$$A = (1/2) \int_{x_1}^{x_2} xdx,$$

which gives

$$A = (1/4)(x_2^2 - x_1^2).$$

Applying this relation for several successive positions of the moving sector, one may secure a number of values which may be plotted. The result can be checked by means of the planimeter. For the particular case in hand the curve shown as Fig. 7 is obtained. The corresponding oscillographic record of this case is given as Fig. 8. It will be seen that the computed and the experimental results are in fair agreement.

To approach the problem from another point of view, suppose that it is desired to produce, by such a device, some definite e.m.f. wave form, say a sine wave. It then becomes necessary to determine in advance what shall be the shape of the electrodes. In the case cited the area must be a sine function, that is,

$$A = B \sin x,$$

where B is constant. Differentiating,

$$dA/dx = B \cos x.$$

In rectangular coordinates area is given by

$$A = \int ydx.$$

Differentiating

$$dA/dx = y.$$

Equating

$$y = B \cos x, \tag{4}$$

which is the equation of the bounding curve of the area which will give the required sine variation in capacitance.

In deriving Eq. (4) it has been assumed that the moving electrode will at some instant completely cover the fixed area. In practice, due to design difficulties, it is more or less impracticable to have the moving electrodes as large as the fixed area; a narrow rectangle is accordingly employed as the rotating element. This does not however change the basic relation.

In Fig. 9 successive areas of the rectangular electrode as it moves over the area under a cosine curve are plotted against displacement. Fig. 10 is an oscillogram of the e.m.f. curve actually secured. Fig. 11 is a record of the e.m.f. from the same two electrodes when the film traveled at a slower speed. The freedom from harmonics is to be noted.

It will be noted that the curve is not entirely symmetrical. During the course of the experimental development of the electrostatic generator it was

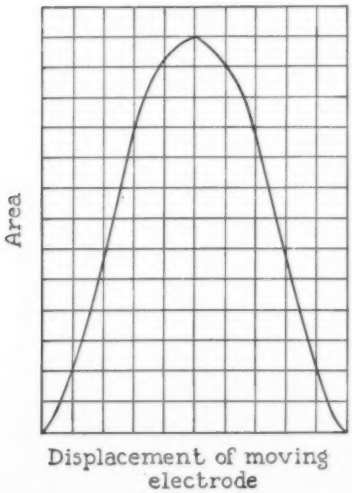

Fig. 9. Area as a function of relative displacement of electrodes shown as *b*, Fig. 6.

Fig. 10. e.m.f. wave form given by electrode system *b*, Fig. 6.

Fig. 11. Same as Fig. 10 except slower film speed.

found that very slight irregularities in the curvature of the electrodes produce appreciable effects in the wave form of the e.m.f. The same may be said in regard to irregularities of the edges of the areas, though to a lesser extent. It was observed that practically all departures from wave symmetry could be traced to a lack of mechanical symmetry.

Other than Sine Waves

In order to illustrate the fact that e.m.f. waves of various forms may be produced by this form of generator an area of the character designated as *C* in Fig. 6 was used. It is to be noted that this area is nonsymmetrical with

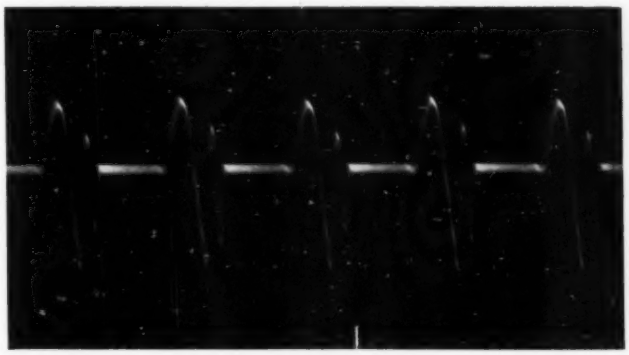

Fig. 12. e.m.f. wave form given by electrode system *c*, Fig. 6.

respect to the *Y*-axis. Fig. 12 shows the record of the e.m.f. resulting from the relative movement of the electrodes referred to. The e.m.f. plainly follows the occluded area and a complex wave form results. In this, as in all cases, whenever $dc/dt=0$, the current flowing into or out of the condenser *C*

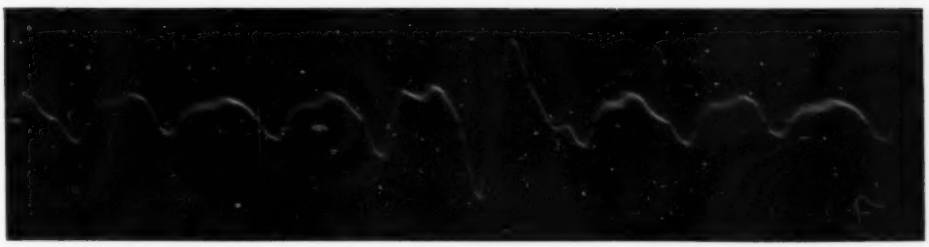

Fig. 13. e.m.f. forms given by various electrodes on same rotor.

(Fig. 2) is zero and hence the e.m.f. developed by this organization is zero. Bearing in mind this and the other relations which obtain it is possible, by proper design of areas, to produce practically any desired wave form. Fig. 13 is an oscillographic record of the waves resulting from the use of several different combinations of electrodes, and illustrates the possibilites of this device.

Limitations

So far as the production of an e.m.f. having a pure sine wave is concerned the tuning fork electrostatic generator will give excellent results, providing a satisfactory method of exciting the fork can be devised. The common model of electrically driven fork will not answer, as the fork in such a case does not vibrate in a simple manner. Oscillograms of the e.m.f. developed from such a unit discloses the presence of numerous harmonics. Work is being carried forward on the production of a method of excitation which will result in simple harmonic vibration of the fork.

In the case of the rotating electrostatic alternator a new model is being constructed which will incorporate the results of experience thus far gained. The most important change in the design is the use of larger capacitance areas, thus reducing the effects of mechanical irregularities. In the new design the moving electrodes will, of course, be so spaced that the generator will yield a continuous series of curves.

Conclusions

From the foregoing discussion it will be evident that it is possible to assemble a comparatively simple and inexpensive electrostatic e.m.f. generator whose wave form will be a pure sine curve, and that other desired wave forms may be also produced at will.

The author desires to acknowledge the assistance rendered by Mr. Philip Nason in the experimental aspects of this investigation.

The Mechanics of Effervescence

By Otto Stuhlman, Jr.
The University of North Carolina

(Received March 19, 1932)

Bubbles of gas when released in a liquid, at depths great compared to their diameters, on reaching the surface burst and eject droplets of the fluid into the air. Each bubble whose diameter is less than the critical value, on bursting simultaneously ejects many droplets. As many as seven droplets were observed for pure freshly-surfaced water at 21°C for bubbles less than 0.12 cm in diameter, for benzene as many as four at 22°C when bubble diameters were less than 0.15 cm. For the same diameters maximum heights of 14.0 cm and 9.0 cm were found for water and benzene. Bubbles having diameters less than 0.10 cm eject droplets to heights which are proportional to the three-halves power of the radius. Bubbles having greater diameters than those mentioned as critical, burst with less regularity, but always project larger droplets to lesser heights as the diameter increases. This irregularity is attributed to instability of the rising bubble. The height distribution h of the droplets at any single explosion is found to vary with the number n so that log h decreases proportionally as n increases. If a large number of droplets at a given height is examined for variation in distribution it is found that a sharp lower boundary exists but a more straggling distribution for the larger values of height. An analysis shows this to be approximately a Maxwellian distribution. The bursting bubble is accompanied by a gas vortex ring ejection, which assists in raising a liquid jet and stretching it beyond its stable configuration until it breaks into the exponentially distributed droplets mentioned above. After integrating this exponential drop distribution with respect to the integral number of drops observable it was found that the reconstructed jet had the form hx^2=constant. Because of the microscopic form of the jet no quantitative measurements could be made so that the converse case was considered, namely the jet produced by the reaction of a falling drop on a liquid surface, as presented by the photographic results obtained by Worthington. His jets when analysed as to volume gave the same mathematical expression as the one found from the data cited above. This reconstructed picture is offered as the solution of the mechanics of effervescence.

THE fact that solutions of many substances foam at certain concentrations is well known and to produce this foam, bubbles of gas may be formed in the liquid naturally or artificially. The control of the stability of the bubbles forming the foam is an important and, as yet, only partially solved technological problem. The mechanics of the bursting bubble and its accompanying ejection of sprayed particles of liquid is the particular phase of the problem presented here.

It is well known that a very small bubble of gas rising in a liquid attains a terminal velocity proportional to the square of its radius. This characteristic behavior of small bodies moving in a resisting medium was quantitatively formulated as early as 1880 and is known as Stoke's law. H. S. Allen[1] raised the question of the validity of Stoke's law as applied to bubbles of large

[1] H. S. Allen, Phil. Mag. **50**, 323 (1900).

diameters, since with increase in radius the terminal velocity of a rising bubble should increase without limit as the size of the bubble is increased. Allen found that for bubbles varying in diameter from 0.00471 to 0.0380 cm the terminal velocities were, however, only proportional to their radii.

The same objection was later raised by Miyagi[2] to Allen's linear relation. Hence he extended the investigation of the terminal velocities of natural and artificial bubbles issuing from capillary openings to bubbles having diameters as great as 0.70 cm. Miyagi, however, accepted the linear relation found by Allen as applying to bubbles having diameters lying between 0.04 and 0.24 cm. For bubble diameters varying between 0.34 and 0.50 cm he finds that the terminal velocities may best be represented by a relation in which this velocity is proportional to the square root of the radius of the bubble.

The composite results may, therefore, be expressed by a relation in which the terminal velocity as a function of the radius rises initially very rapidly, then gradually attains a maximum and drops off parabolically for relatively large bubble radii. Miyagi attributes the departure from the linear relation for values of diameters greater than 0.34 cm as indicating instability in the bubble motion.

He draws an additional important conclusion from his work which has a direct bearing on the problem under discussion, namely that any artificial bubble reaches its terminal velocity almost as soon as it leaves the nozzle above which it is formed.

Behavior of Bubble at Interface

If a bubble of gas or vapor were released in a liquid at a depth great compared to its diameter, it would rise and very rapidly attain its terminal velocity and, as Miyagi[2] has shown, continue to ascend in a helical path, keeping its shape flattened in the direction of its motion. In making the following observations it was found that for very small bubbles the helical pitch was very large so that the bubbles arrived at the interface with small horizontal velocity components which for all but very minute bubbles makes them skid along the lower surface of the interface before coming to rest and bursting. If the interface has the same molecular structure as the body of the liquid, or, as in the case of a freshly formed surface of a solution, it possesses the same concentration of solute as the body of the liquid, the delay in bursting caused by the skidding is negligibly small and the bubble seems to burst immediately upon its arrival at the surface. If, however, the interface has, as a result of aging or contamination, taken on the properties of a monomolecular film, the delay in bursting may be very great, even resulting in foam formations.

The bubbles in bursting project numerous droplets of the liquid vertically upward. Slight horizontal air currents produce the usual type of parabolic trajectories. As the diameter of the bubble is increased the size of the ejected droplets also becomes correspondingly larger. These sprayed particles rising above the surface of the liquid were first examined for height distribution

[2] O. Miyagi, Phil. Mag. **50**, 112 (1925).

and either observed through a cathetometer or photographed, under the following conditions.

Technique

Artificial gas bubbles were formed at the end of a very find glass capillary, placed about 10 cm below the surface of the liquid. Although no constant temperature bath was used for the liquid, an acceptable series of observations did not show a temperature variation in excess of one half a degree centigrade. The diameters of the bubbles were measured just at the moment of release. The gas was obtained from a storage reservoir kept at a constant pressure.

The ejected droplets, from the bursting bubbles, were illuminated with a 1000-watt projection incandescent bulb placed behind a 23 cm condenser lens. The beam of light was focused on the bursting bubble and ejected droplets. The cathetometer or camera was set for maximum brilliancy of illumination at an angle equal to the critical angle of the liquid under examination.

It was found that at each burst several droplets were ejected to distinctly differing heights. For small bubbles as many as seven droplets could be observed, not counting the splashes from the descending shower. The number, the distribution in height, and the volume of the ejected droplets varied with the size of the bursting bubble. Unless otherwise specified the data to be presented were all taken with pure, freshly surfaced liquids, free from known surface contamination.

Height as a Function of Bubble Diameter

The cathetometer observations indicated that the individual droplets were always projected, on the average, to the same height for a given bubble diameter. The departures from any mean height were found to be consistently different for those above, as compared with those below this value, so that a form of skew probability distribution was suspected, and photographically verified.

Figs. 1 and 2 show the results obtained from water and benzene. Heights of the ejected droplets are represented as a function of the radii of the bubbles producing them. The heights were observed with a cathetometer and represent the most probable values of a large group of observations. These two liquids were examined with a view of showing the behavior of the ejected droplets as possibly influenced by a difference in molecular structure, surface tension, viscosity or physico-chemical properties of the liquids. Water was chosen because of its unsymmetrical molecular structure, and the possible influence of the hydrogen atoms at the interface supposedly orientated towards the vapor phase,[3] benzene because of its non-associated and more symmetrical structure with surface energy almost twice that of water.

The outstanding features of these two curves is that maximum heights of ejection are just about twice as great for water as for benzene. Each bubble

[3] W. D. Harkins, Colloid Symposium Monograph **II**, 141 (1925).

explosion is accompanied by the simultaneous ejection of several droplets. For water as many as seven separate particles were observed ejected by bubbles having diameters in the neighborhood of 0.075 cm. The height of ejection rapidly attains a maximum for both liquids, from which value sub-

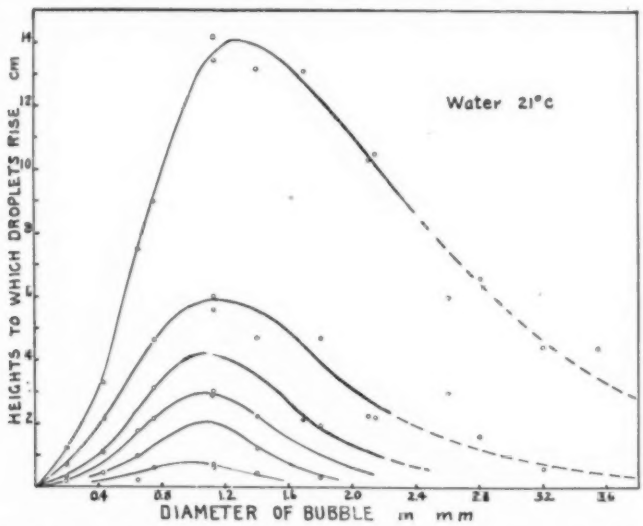

Fig. 1. Shows distribution of effervescing droplets above a pure water surface, for single bursts of bubbles with increasing diameters. Air bubbles were generated at 5 cm depths and increasing bubble diameters were obtained by means of changes in diameters of capillary tube openings. Note scattered results as bubbles approach instability, beyond the maximum.

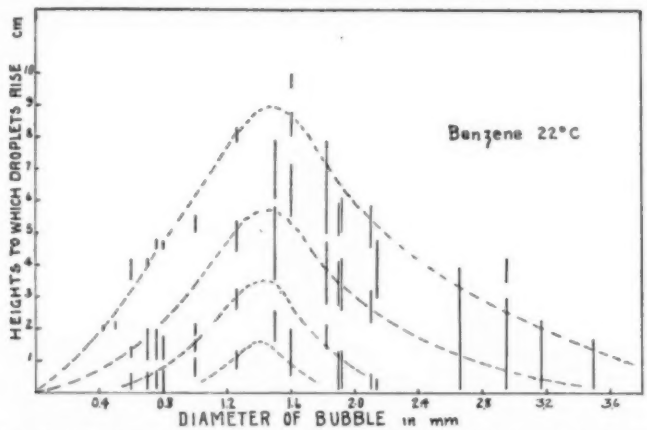

Fig. 2. The distribution in height of droplets of a single bubble with increased diameter. Air used to produce bubble. Note the instability as compared with water. Vertical lines show range in which the averages of a large number of observations were located.

sequently it gradually drops as the bubble diameter gets larger. It will be noticed that after the maximum or critical value of bubble diameter is past, the number of ejected drops accompanying a burst grows fewer. It was also found that as the bubble diameter increases the size of the drops becomes larger.

The results obtained for benzene were less accurate than those for water, as indicated by the vertical bars which are used to locate the range of the height. This was primarily due to the unusual volatility of the liquid, which tended to exaggerate the heights. Slight horizontal air currents also tended to distort the paths into narrow parabolic trajectories. No corrections were made for this loss in height. Distorted trajectories were omitted in the final analysis.

In the case of water the maximum height attained by the droplets was 14.0 cm, when the bubble diameter was 0.12 cm. The gas was air, the temperature of the fluids was 21° C. For benzene a maximum height of 9.0 cm was attained at 22° C from a 0.15 cm bubble. A bubble having a diameter corresponding to the maximum height of ejection of water, in the case of benzene, attained a height of only 7.6 cm. From this evidence it is concluded that surface energy is apparently the dominant factor in a rather complicated sequence of events controlling effervescence.

For bubble diameters greater than 0.24 cm the curves are shown as broken lines indicating that the ejection of the droplets was not of sufficient regularity to warrant quantitative interpretation. An explanation of the erratic behavior of the bursts is found in Miyagi's[2] conclusion that bubbles having a diameter greater than 0.3 cm are unstable.

The initial rise in the curve can, however, be interpreted quantitatively. For bubbles having diameters less than 0.10 cm the height of ejection is very accurately proportional to the three halves power of the radius. It is in this region that Miyagi found the velocity of the ascending bubble to be perfectly stable.

Height Distribution of Droplets

One of the dominant characteristics of the bursting bubble is the simultaneous ejection of several droplets of liquid. As many as seven droplets can be observed for bursts due to bubbles less than 0.14 cm in diameter. Fig. 3 shows the linear relation obtainable when the logarithm of the height h is examined as a function of an integral number n ascribed to the successive drops originating from a single burst. Hence

$$\log h = \log b - cn$$

where $c = \log b/a$. Where h and n are so related that when the droplets, here assumed as of equal volume, are taken in an arithmetical series, the corresponding values of the height to which they are ejected above the liquid surface, forms a geometrical series.

If instead of examining the results from a single burst we photographically record the trajectories of several hundred bursts, for a given bubble radius at constant temperature, we find that the heights found for a single group do not distribute themselves according to the probability function. Such a height distribution amongst the top group of ejected particles is represented in Fig. 4. It will be noticed that the curve is, to all appearances, a Maxwellian distribution.

In order to examine the results, we can imagine a collector placed above the surface out of range of the highest droplet and gradually lowered. The number reaching the collector as it approaches the surface of the liquid at millimeter intervals can be obtained by integrating the data of Fig. 4. These integrated values are represented in Fig. 5 curve *A*. The result takes the form of a typical distribution curve as associated with photoelectric and thermionic emission phenomena, when surface contamination distorts the electron energy distribution. The pronounced sharp upper knee shows that there is a sharp lower level to the cloud of droplets associated with any height *h* and that relatively few droplets are found at heights less than the most

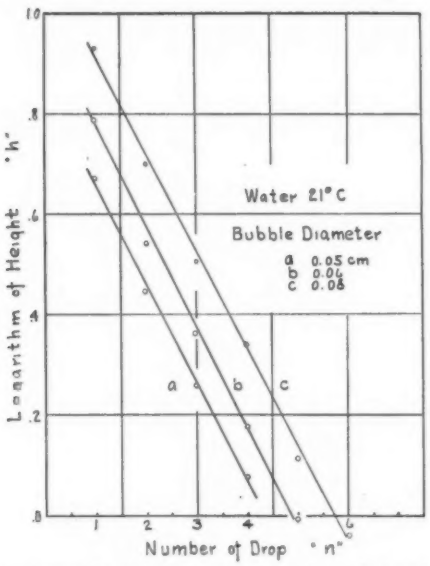

Fig. 3. This shows the logarithmic height distribution of the droplets associated with a single burst, for various bubble diameters in the region of greatest bubble stability.

probable height. The foot of the curve shows that the droplets which occasionally exceed the most probable height are more numerous and straggle along as in a Maxwellian distribution. How much the above distribution departs from a Maxwellian law is shown in Fig. 5 curve *B*. It will be noticed that the lower edge of the cloud of droplets is very sharply defined, curve *B–S* so that the Maxwellian curve *B–M* is skewed to the left, making ejection for any given height more monochromatic than a Maxwellian distribution predicts.

Source of Ejected Droplets

With the above analysis in mind it is possible to reconstruct the mechanism of the bursting bubble followed by the ejection of a series of droplets with their unique logarithmic height distribution.

The rising bubble arrives at the interface with its characteristic terminal velocity. If the interface possesses a molecular structure in no way differing from the body of the liquid, the bubble bursts immediately. If, however, the

interface is composed of a monomolecular film, a delay in bursting results. This delay may be increased to such an extent that a more or less stable foam is produced. The bursting of these foam bubbles does not produce the spray described in the above effervescence experiments. In the former case a very rapid sequence of the following events should take place.

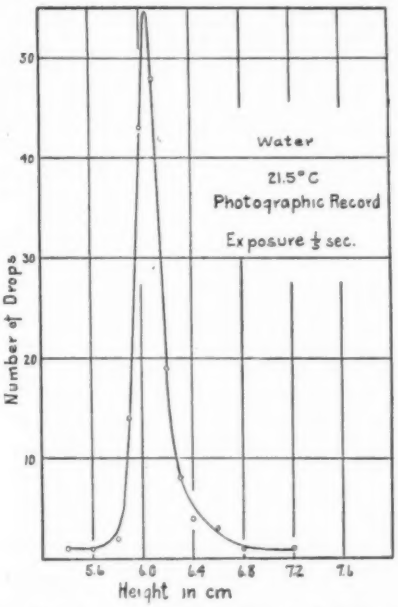

Fig. 4. A composite record, photographically obtained at one exposure. Shows the variation in height of the uppermost droplet level during one fifth of a second. The most probable height is 6.05 cm. Bubble diameter 0.0056 cm. Here terminal velocity is proportional to radius.

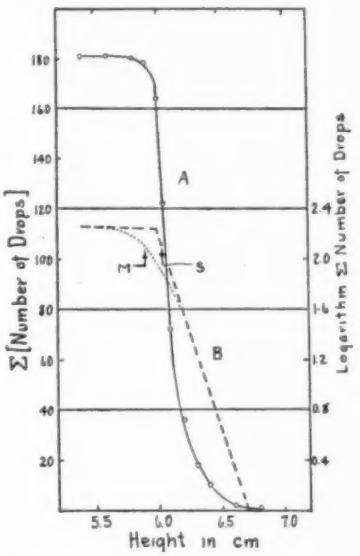

Fig. 5. Curve *A*. Shows the usual type of distribution curve obtained by integrating the results of Fig. 4. Note the relatively abrupt change in height indicated by knee as compared with foot of curve. Curve *B*. Shows the results obtained when the logarithmic values of curve *A* were replotted as a function of height. The point *S* shows the location of the most probable height as compared with the most probable height *M* if the distribution were Maxwellian.

Since uniformity of concentration or molecular symmetry in the surface layer and body of the liquid can be assumed to exist only when the surface layer is freshly formed, it follows that after any appreciable length of time we may consider the surface as already possessing the characteristics of a monomolecular film having surface elasticity. This surface film must, according to the Langmuir[4] surface structure theory, have a "characteristic architecture" and in the case of water, as pictured by Harkins,[3] the hydrogen atoms must be turned towards the vapor and the oxygen to the liquid phase. The air bubble, even after a rapid ascent through the water, must arrive at the interface possessing a similar polarized surface structure.

The bubble must, therefore, pause just long enough at the interface to allow the water to drain from between these monomolecular surfaces. This

[4] I. Langmuir, J.A.C.S. **39**, 1884 (1917).

draining takes place less rapidly the greater the radii of curvature of the surfaces. The draining continues until a dark spot is formed at the top of the bubble. Rupture of the bubble takes place at this point.[5] The circular opening thus formed suddenly releases the gas inside of the bubble. This explosive release of the gas through the circular opening takes the form of a vortex ring.[6] Such vortex ring formations, due to exploding bubbles, were originally observed by W. B. Rogers[7] who describes the changes in this vortex motion in great detail.

The bubble is subsequently destroyed by a progressive enlargement of the opening due to excessive evaporation at the cusped edge forming the lip of the opening. The enlargement of the opening must, however, take place with sufficient slowness to allow the aperture to give direction to the gas blast forming the vortex ring. The vortex ring rising in a resisting medium with decreasing speed progressively expands as it rises. Since the volutes of the ring gather air into their folds from the inner section of the ring it follows that this inner section with its lowered pressure must assist in drawing the liquid projected from the bottom of the bubble into a volcano-like jet.

This concave surfaced liquid jet is the source of the drop formation following the bubble explosion. The jet continues to rise and eventually is stretched sufficiently to form an unstable column of liquid which breaks into drops. It should, therefore, be possible to reconstruct the figure of the jet by integrating the logarithmic droplet distribution found from Fig. 4.

As early as 1873 Plateau[8] had shown that a liquid cylinder is not a figure of stable equilibrium if its length exceeds π times its diameter. Such a jet breaks into drops of equal volume for every π times the diameter of the jet. The distance between such drops is uniform and equal to the circumference of the cylindrical jet.

The logarithmic distribution of the droplets found in these experiments should not, therefore, lead us to a reconstructed jet of a cylindrical form.

Jet Form

From the data shown in Fig. 3 and similar results obtained from the distribution in height of the individual droplets emitted simultaneously from a single burst it was found that

$$\log h = \log b - cn$$

where $n = 1/c(\log b - \log h)$. Let each of the drops have a volume V. Then the reconstructed jet composed of n droplets has a volume

$$Vn = \frac{V}{c}(\log b - \log h).$$

[5] R. E. Wilson and E. D. Ries, Colloid Symposium Monograph **I**, 145 (1923).

[6] Campbell, Swinton and Beale, Nature **98**, 469 (1917).

[7] W. B. Rogers, Amer. Jour. Sci. **26**, 246 (1858).

[8] J. Plateau, Statique, expérimentale et théorique des liquids sourmis aux seules forces molécularies. Gent 1873.

The problem then reduces itself to finding the curve which when revolved about the vertical axis h, will have the given volume. Hence

$$-\pi \int_h^{h_0} x^2 dh = \frac{V}{c}(\log b - \log h)$$

and

$$\pi x^2 = V/ch \quad \text{when} \quad h = 0, \; x = \infty$$

therefore

$$hx^2 = \text{constant}$$

is the desired volume.

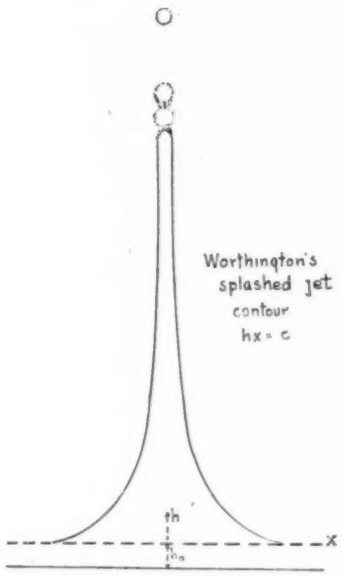

Fig. 6. A scale reproduction of one of Worthington's splashed jets. Taken from his *Study of Splashes.*

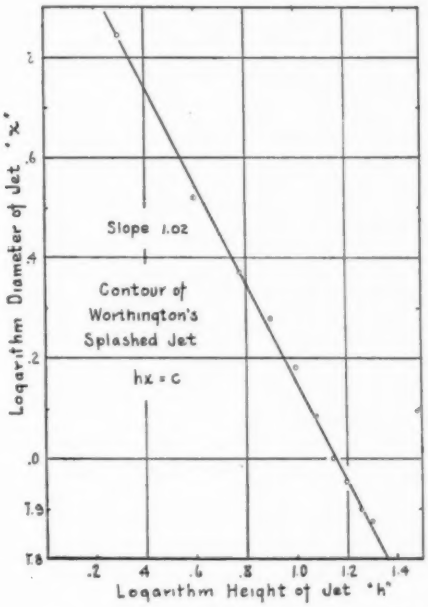

Fig. 7. Shows the relation between the height of the jet and its diameter. The upper end, however, approaches a cylindrical form.

Experimental Evidence for this Jet Form

The jets ejected by the bubbles were too small to photograph, so we must look for an indirect experiment that can be used to prove that the jet under similar conditions is of the form derived above.

For this purpose the converse situation was considered. On a larger scale a similar jet is generated by allowing a large drop of water to fall from a height on an undisturbed water surface. The splash thus formed is accompanied by a jet due to the reaction of the circular depression, formed by the descending drop. A similar phenomenon can be produced by directing a current of air downward against a liquid surface and then suddenly interrupting the flow of air. C. W. Foulk[9] observes that the depressed area flies up and the necking off of the projected droplets can be observed.

[9] C. W. Foulk, A.S.M.E. **14,** Nov. 30 (1931).

In view of the beautiful experiments by Worthington[10] and the exceptional clarity of some of his photographic reproductions, showing the progressive development of a splash due to a falling drop with the resulting jet formation, it was thought more desirable to analyse these photographic records in preference to new records that could be made under similar circumstances. While it is admitted that this argument by analogy is logically the weakest link in the analysis, it should however, lead to a qualitative solution of good approximation.

The splash shown in Fig. 6, taken from Worthington's illustrations, was chosen and reproduced because it showed to the best advantage, not only the formation of the jet but also the position and distribution of the droplets at the top of the jet. The photograph was projected with twentyfold magnification on a white sheet of paper and carefully copied. The height of the jet was divided into two centimeter sections and the diameter of the jet was measured at these sections. Fig. 7 shows the results obtained by plotting log radius as a function of the log height of this jet. The straight line thus obtained has a slope equal to 1.02. The contour of the jet is hence $hx = \text{constant}$. Integrating this relation between the limits h and h_0 then for values of $h = 10\ h_0$ as shown here, the volume generated is $V = 18\pi hx^2$, a form similar to the one arrived at from our experimental data.

An additional point of interest is that in Fig. 6 the jet is seen to be in unstable equilibrium because droplets are necking off. The highest droplets have separated themselves from the jet and readily show the nonlinear distribution in height demanded by the above theory. Whether the distribution is exponential could not be determined with sufficient accuracy, since not enough photographic data were available.

The two phenomena are, therefore, at least as to the form of the jet, quantitatively similar and present a qualitative resemblance to each other as far as the distribution in height of the separated drops is concerned. Thus at least an acceptable mechanical picture is presented of a bursting bubble and the manner in which it can produce the necessary observed spray ejected from the surface of the liquid as found in effervescence.

I take pleasure in acknowledging the assistance of my former students: H. H. zur Burg, K. Z. Morgan, C. J. Craven, and H. B. Mulkey, who participated at various times in this investigation.

[10] A. M. Worthington, Phil. Trans. Roy. Soc. **A194,** 198 (1900). Study of Splashes. Longmans 1908.

The Size and Size Distribution of Fog Particles

By H. G. HOUGHTON
Round Hill Research Division, Massachusetts Institute of Technology

(Received March 23, 1932)

An apparatus for the microscopic measurement of fog particles is described. The particles were collected on a slightly greased glass slide and viewed with the aid of dark-field illumination. The particle sizes were measured either visually with an eyepiece micrometer or, more usually, by the subsequent measurement of photomicrographs. With the aid of this apparatus a series of fog particle size distribution curves were obtained. These curves are characterized by a single maximum which always occurs at a particle diameter which is an integral multiple of 3.1 microns. The curves approach the axis asymptotically for large particle diameters but have a definite minimum. An explanation for this minimum on the basis of certain properties of the nuclei of condensation is offered.

IN A recent theoretical investigation it was found that the transmission of light through fog was dependent on the particle size and size distribution as well as on the density or number of particles in a unit volume.[1] The literature on the subject of fog particle size was found to be very incomplete especially with regard to the size distribution. Köhler[2] has probably made the most extensive particle size measurements but with the exception of a few microscopic measurements of frozen drops and drops on wires his results have been derived from corona measurements which give only the predominant particle size. His deductions as to the size distribution made from these data are therefore the variations of the predominant size with time rather than an instantaneous distribution such as is desired.

Wells and Thuras[3] obtained an average particle diameter of ten microns for sea fogs by a somewhat involved and indirect method. Barus[4] and Werner[5] have also made some corona measurements in artificial fogs. Anderson[6] has measured some of the particles of his artificial fogs and the author[7] has made some rather unsatisfactory microscopic measurements in some small particle artificial fogs.

It was felt that more definite and detailed data were essential not only for the work on the transmission of light but also for any problem dealing with fog. It was the purpose of the work described in this paper to develop the necessary apparatus and methods of measurement and to collect suffi-

[1] J. A. Stratton and H. G. Houghton, Phys. Rev. **38**, 159 (1931).

[2] Hilding Köhler, Hydrografiska Anstalt 2, No. 5, Stockholm 1925; Meteorologische Zeitschrift **40**, 1923; **42**, 1925.

[3] P. V. Wells and A. L. Thuras, U. S. Coast Guard Bulletin No. 5.

[4] C. Barus, Am. Jl. Sci. **175**, 224 (1908).

[5] O. Werner, Ann. d. Physik **70**, 375, 480 (1923).

[6] S. H. Anderson, Trans. A.S.M.E. **4**, No. 1 (1932).

[7] H. G. Houghton, Phys. Rev. **38**, 152 (1931).

cient data to determine the particle size distribution of such natural fogs as were available. The measurements were made at Round Hill, South Dartmouth, Massachusetts, which is situated on the west shore of Buzzard's Bay about six miles south of New Bedford.

In order to permit the work of developing the apparatus and methods of measurement to proceed when there were no natural fogs, a chamber was built in which artifical fogs could be produced by the rapid expansion of saturated air. The fog chamber was constructed of heavy wood lined with copper and was airtight. It contains a fan for circulation, a series of wicks to humidify the air and a heater to obtain the desired temperature. The fog is formed by increasing the pressure to about ten pounds per square inch above atmospheric, saturating the compressed air and then allowing it to expand rapidly to atmospheric pressure. The temperature drop due to the expansion causes the condensation and by properly regulating the initial temperature the fog can be formed at room temperature and is very stable.

Although it is possible that the corona method could be extended to give a size distribution, the direct microscopic measurement of individual particles seemed to offer more possibilities. Direct measurement of the particles while they are suspended in the air is extremely difficult due to their rapid motion. This motion can be reduced by confining some of the fog in a small chamber below the objective as has been done in previous measurements,[7] but it seems possible that the larger particles would settle out before measurements could be made. Any method for the measurement of fog particles while suspended in the atmosphere would have to be entirely photographic and it has been estimated that an exposure of about one-hundred-thousandth of a second would be required to stop the motion of the particles. It did not seem practical to obtain the illumination which would be necessary for this method and it was decided to observe the particles at rest on a glass slide. This method is by no means completely satisfactory as will appear below but it does give results of definite value which are reasonably accurate.

Since the fog particles are transparent it is necessary to use dark-field illumination. With this type of illumination the drops appear self-luminous against a dark background. There are several forms of dark-field illuminators on the market but they were not entirely satisfactory for this application and a special illuminator was constructed. A direct current carbon arc was chosen as the light source because of its high intrinsic intensity and small size. The positive carbon was mounted horizontally and a shield placed to eliminate the image of the negative carbon. Light from this source is collected by a large, short-focus collimating lens. The resultant parallel beam then passes through a water cell, which is very necessary because the heat of the arc would almost instantly evaporate the small fog particles. To reduce further the heat on the slide a foot-operated shutter was placed in front of the arc so that the particles are illuminated only while under observation. The microscope and the dark-field illuminator are vertical and the parallel beam is turned in this direction by means of a mirror. The dark-field illuminator proper consists of a series of three achromatic lenses mounted

in a bakelite tube which may be readily removed from the apparatus for cleaning or replacement. The dark field was obtained by placing opaque disks on the lenses of such a diameter that the angular aperture of the resultant dark cone was slightly greater than the aperture of the objective. No direct light enters the objective and the field is dark. The object slide is at the focal point of both the objective and the illuminator and a drop in this position appears brightly illuminated due to the scattered light. The slide holder was constructed so that the slide could be readily moved from

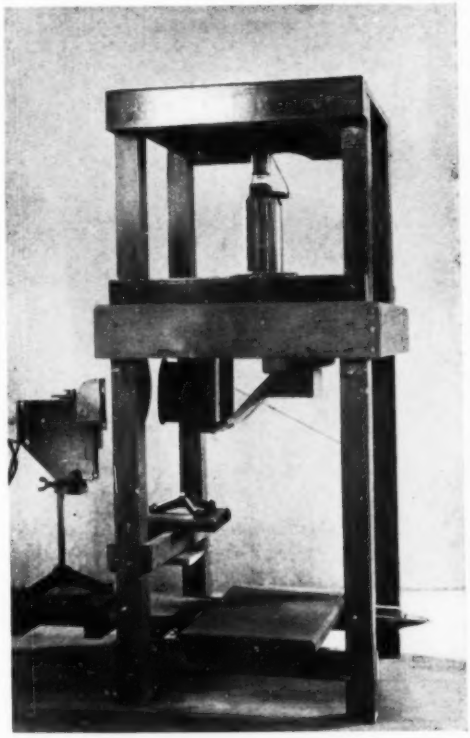

Fig. 1. View of the complete apparatus for the microscopic measurement of fog particles.

underneath the objective and out into the air to collect fog and then pulled back for observation. This movement is controlled by conveniently located cords. When in position for observation the slide and all of the lenses are completely enclosed in a small chamber which serves to keep the moisture from collecting on the lenses and also acts as a guide for the microscope. A complete view of the apparatus is given in Fig. 1. The upper frame work containing the microscope and the illuminator may be readily removed and replaced by the previously described fog chamber when it is desired to use artificial fogs. The microscope and illuminator are used interchangeably in the open frame and the artificial fog chamber.

The glass slides were the cause of considerable trouble. The ordinary microscope object slides which were tried were very unsatisfactory because of the small surface bubbles and scratches which appeared brightly illuminated. This was not only confusing but it also reduced the effectiveness of the dark field. It was finally necessary to obtain some specially surfaced slides which were practically free from these defects.

In order to keep the drops from spreading on the glass, a small amount of grease must be applied to the slide. Under the microscope the globular nature of the grease is quite apparent and some of the advantage of the special slides is lost. However, by exercising care in the application of the grease it is possible to prevent the drops from spreading and at the same time to maintain a reasonably dark field.

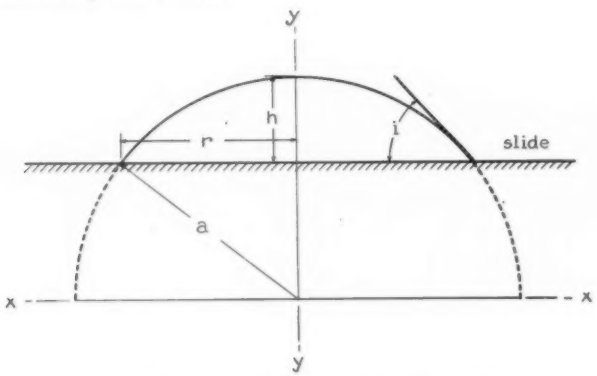

Fig. 2. Diagram of fog particle on a slide.

Although the greased slides prevent spreading, it is apparent that a drop resting on the slide will not be spherical but will be more or less flattened by its own weight. The drop diameter as measured from above will thus be greater than the diameter of the original spherical drop. By reference to Mathieu[8] it was determined that the free surface of drops of the size of fog particles could be assumed to be spherical without introducing an appreciable error. The determining factor is the angle at which the water meets the surface of the slide. Mathieu designates this angle by i and its sense is as shown in Fig. 2 which is a vertical section through the apex of the drop. This angle is a function of the surface on which the drop is resting and is independent of the size of the drop. In view of the importance of this factor a series of experimental determinations of i were made by three distinct methods. In each case the slides were greased in exactly the same manner as those used for collecting the fog particles. In the first method large drops were formed and their height, diameter and weight determined. By assuming that the radius of curvature at the apex of the drop is very large, the angle i may be computed from these measurements. The second method involved the measurement of the height of a capillary column between two slides. The angle i may then be computed from this height, the spacing of the slides and the

[8] Théorie de la Capillarité, Mathieu, p. 142.

surface tension constant. As a final check, the height and diameter of drops of about the same size as the fog particles were measured microscopically. As a result of this series of measurements it was found that i did not vary markedly for slides which were similarly greased. The average value of i as obtained from the three methods was found to be 42°. Taking the free surface as spherical, the volume of the flattened drop may be represented in terms of the measured diameter and the angle i. A simple calculation shows that for $i=42°$

$$R = 0.533r$$

where R is the radius of the original drop and r the measured radius on the slide. The factor 0.533 must be applied to all of the measurements to reduce them to the size of the original spherical drop.

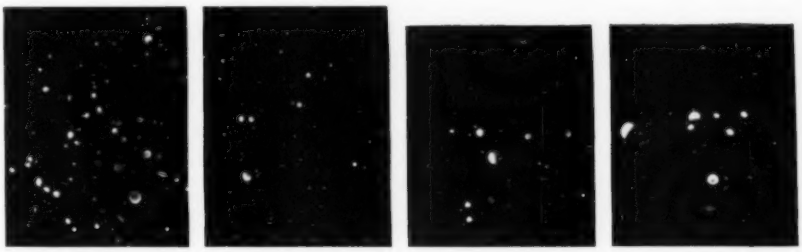

Fig. 3. Photomicrographs of fog particles.

Before any measurements can be made it is essential that the entire apparatus be at air temperature. If it is too warm the drops will evaporate and if too cold they will grow larger or moisture will collect on the slide. If the apparatus is kept indoors it may require as long as two hours for it to reach air temperature.

Because of the relatively rapid changes in the characteristics of fogs it is essential that a sufficient number of measurements for a size distribution curve be made within a short time. It was at first thought that this could be most readily accomplished by visual measurements with an ocular micrometer and a number of fairly satisfactory curves were obtained in this manner. It was soon found, however, that the accuracy of measurement which was consistent with the requisite speed was somewhat below the desired standard. It was, therefore, decided to make photomicrographs which could be measured later with almost any desired accuracy. A projection ocular was not available and the first photographs were made by direct projection of the image of the objective. This method produced rather unsatisfactory photographs because of the saucer-shaped image formed by the objective. It was found that much better results could be obtained by using both the ocular and the camera lenses. This method gave satisfactory results and Fig. 3 is a sample of the photographs obtained in this manner. As many as one hundred and fifty drops were sometimes obtained in a single photograph. Objectives with an initial magnification greater than about ten diameters

were not satisfactory because the decreased depth of focus made it necessary to refocus for drops of different size. If greater magnifications are desired a good negative may be enlarged at least four diameters. Due to defects in the slides and the limit of the resolving power of the microscope, particles smaller than about one to two microns in diameter are not readily identifiable.

It is apparent from an inspection of a large number of fog particle photographs that the particle size is continuously variable. That is, the fogs which have been measured do not consist of discrete groups of particles of the same or about the same size as has sometimes been assumed. In order to obtain a

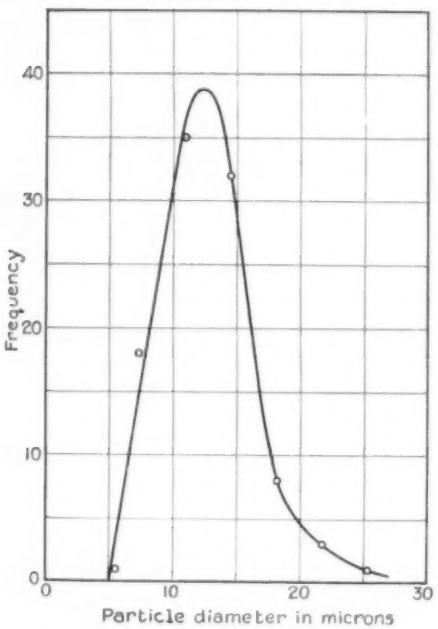

Fig. 4. Size distribution of fog particles at 11:00 A.M. on October 5, 1931. Wind S-10, Baro. 30.15″, Temp. 66°F.

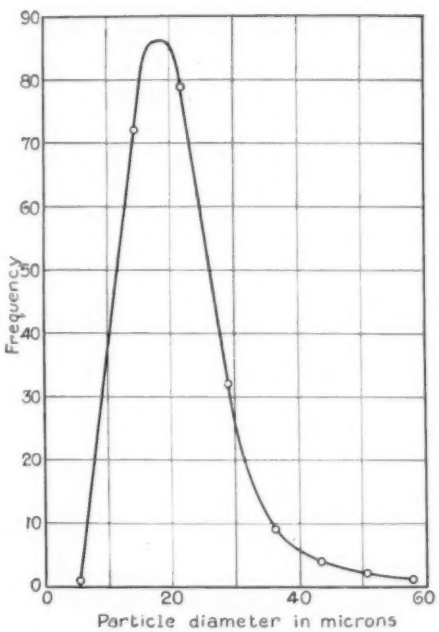

Fig. 5. Size distribution of fog particles at 9:00 A.M. on November 20, 1931. Wind N–7, Baro. 30.50″, Temp. 52°F.

size distribution curve from a finite amount of data, it is necessary to divide the total range of sizes into a number of groups each of which includes a small range of sizes. The number of particles falling within a group is then plotted against a size corresponding to the center of the group. The number of groups depends on the amount of data available and on the accuracy of the size measurements. Since the distribution is a continuous variable, a smooth curve may be drawn through the points. The resulting curve is an approximation to the true curve which it approaches more and more closely as the amount of data and number of size groups are increased. Drop size has been expressed in terms of the diameter because both these and other measurements gave results in this form. For certain purposes the drop volume or surface may be a more logical abscissa but these transformations may readily be made if desired.

Representative distribution curves for the fogs on which measurements have been made are given in Figs. 4 to 7 inclusive. The most obvious and important characteristic, which is common to all of the curves, is that there is a single and very marked maximum. The absence of secondary maxima is an indication that there has been no appreciable combining of the drops. This may be due to the fact that the fog was formed not far from the point of measurement. The location of the maximum varies not only for different fogs but also within a short time in a given fog. Fig. 7 illustrates the progressive and relatively rapid shift of the maximum which is characteristic of the fogs which have been observed. To facilitate comparisons the ordinates

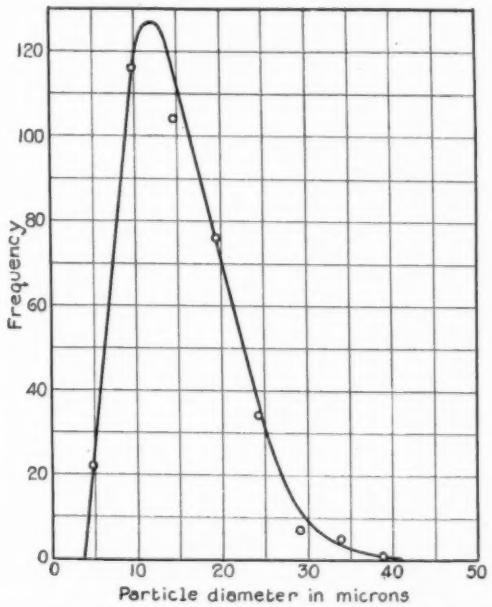

Fig. 6. Size distribution of fog particles at 3:30 P.M. on November 20, 1931. Wind NE–5, Baro. 30.46″, Temp. 54°F.

of these curves have been proportionately reduced so that the maxima have a value of unity. This series of curves illustrates a very interesting and important property of the distribution curves. It will be observed that the three maxima are spaced equally about 3.1 microns apart and that the first occurs at 6.2 microns so that each is an integral multiple of 3.1. This was also found to be true for all of the curves which have been obtained and with the exception of the central curve of Fig. 7 the maxima occur at integral multiples of 6.2 microns. Köhler[2] found a somewhat similar effect but his relation was linear with respect to drop volume rather than diameter. Maxima have been observed from 6.2 to 43. microns, the most common being 6.2, 12.4 and 18.6. Representative curves of these types are given in Figs. 4 to 7. This integral relation undoubtedly has an important bearing on the subject of fog formation but sufficient data are not yet available to correlate these results with the pertinent meteorological factors.

The distribution curves evidently become asymptotic to the axis for large particle sizes but it will be noted that there is apparently a definite lower limit of particle size. This is not conclusive in the case of the smaller particle fogs of Fig. 7 because of the limit of accuracy of the measurements but the existence of this definite minimum in the curves of Figs. 4, 5 and 6, can hardly be questioned. A plausible explanation of this characteristic of the curves may be derived from certain properties of the nuclei of condensation. If the nucleus is neutral and nonhygroscopic the degree of supersaturation at which condensation will take place is dependent on the curvature of the surface of the nucleus. Thus, if nuclei of various sizes are present and supersaturation occurs, condensation will take place only on those nuclei

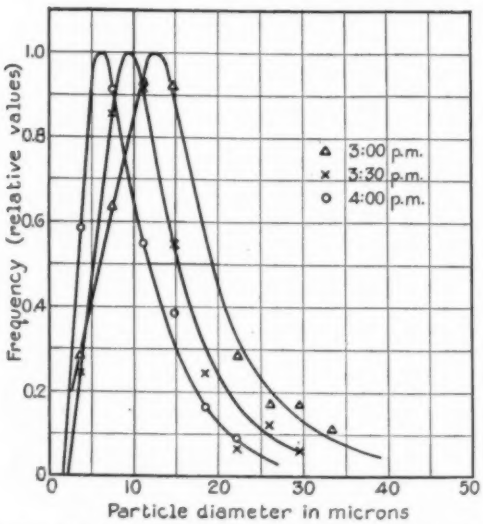

Fig. 7. A series of distribution curves taken at half hour intervals on December 14, 1931. Wind WSW 10 to 20, Baro. 29.57", Temp. 50°F.

which are larger than a certain minimum size which is a function of the initial degree of supersaturation. There is considerable experimental evidence that the nuclei of the fogs which have been observed consisted principally of sea salt which is somewhat hygroscopic because of the small amount of magnesium chloride which it contains. The hygroscopic action partially overcomes the vapor pressure and permits condensation to occur at lower degrees of supersaturation or even at slightly less than saturation. For the moderately hygroscopic sea salt particles there is still a minimum size of nucleus on which condensation can take place as discussed above and this seems to be a reasonable explanation for the observed sharp lower limit of the curves. It is probable that this effect would be less marked or entirely absent in fogs formed on the extremely hygroscopic nuclei which are produced in great numbers in the air around cities as a product of combustion.

The nuclei which are larger than the minimum size will produce fog drops of a size approximately proportional to the size of the nucleus. The upper

portion of the curves which have been obtained should, therefore, also represent the distribution of nuclei sizes greater than the minimum size. The salt nuclei are presumably formed by the evaporation of spray and it is reasonable to suppose that a random distribution of sizes would result. In Fig. 8 a Gaussian or normal distribution function of the form $y = Ke^{-cx^2}$ has been fitted to the upper portion of the curve of Fig. 6. The divergence from the observed data is quite marked to the left of the maximum as would be expected from the above discussion.

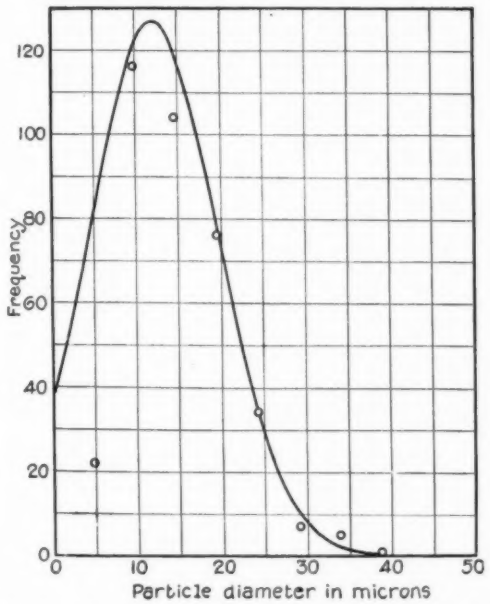

Fig. 8. A Gaussian or normal distribution curve fitted to the upper portion of the curve of Fig. 6. The circles represent the observed points.

The results which have been obtained can be considered only as a beginning of what promises to be an extremely interesting and fruitful study. More data of the same type are desirable in connection with information on the nuclei of condensation and various meteorological factors. It will also be desirable to have similar data on inland and city fogs. It is felt that only a complete study of this sort can hope to offer a real solution to the various phases of the fog problem. A workable method of size measurement has been developed and it has been found, for the fogs which have been studied, that the instantaneous particle size distribution curve has a single maximum which invariably occurs at a particle diameter which is an integral multiple of 3.1 microns. Preliminary explanations for the characteristic shape of the curves have been offered especially for the definite minima of the curves.

For the benefit of those who may wish to draw additional conclusions from the distribution curves the wind velocity, air temperature, and barometric pressure as well as the time and date have been indicated. It may also be noted that Round Hill is a point on the shore of Buzzard's Bay and winds from the west-south-west through south to north-east come from the Bay.

THE EDITOR'S COLUMN

The Physical Theory of Valence

THE application of quantum mechanics to the theory of chemical combinations continues on apace with promise of becoming a strong tool in the hands of the chemical theorist.[1]

What holds molecules together; why do some combinations form stable arrangements while others do not? These are the broad general questions which one desires to answer, but before he can proceed to the answers he must first consider just what is implied in the terms *hold together* and *stable arrangements*. It is obvious from daily experience that all substances do not show the same degree of stability when subjected to disturbing influences such as heating, chemical action, electrical discharge, etc., etc. Stability is a relative idea and cannot be defined in an unambiguous manner; the stability of a given molecule depends upon the characteristics of the various influences which tend to disrupt it. In the broad sense of every-day experience one considers a compound as stable if it exists under fairly diverse physical circumstances; i.e., within a reasonable range of pressures and temperatures. If one considers stability with respect to chemical reactions then the term becomes even more vague, as many *physically* stable substances are easily broken down by chemical means, for instance the rapid corrosion of metals by acids. Clearly this leaves considerable leeway in the definition of stability as applied to any specific molecular group, and it is possible that under proper conditions a certain degree of stability could be imputed to almost any molecular grouping.

As actually applied in discussions of stability there is ordinarily not much doubt as to the meaning of the term. This is because the important problem is usually not the prediction of the stability or instability of an *unknown* molecule, but rather the explanation of the stability of molecules which are known to occur under some given set of circumstances, and which consequently are known to be stable in this sense. An example of a borderline case of considerable importance is that of the relatively loose combinations of ions and molecules in the air forming the *ion clusters*. Though one hesitates to designate these clusters as chemical combinations they are sometimes quite stable.

WHILE the chemical theories of valence have been developed and used for many years, the physicists did not really come into the field until the establishment, for quite different purposes, of the quantum mechanics. Even at present the *physical* valence theory is in a comparatively early stage of development and is mainly concerned with making its peace with the extant chemical theories. It is perhaps not fair to imply that the theoretical quantum mechanics is alone responsible for this common endeavour of chemists and physicists, for this is made possible only through the vast amount of experimental and semitheoretical work which has been involved in the unravelling of the spectra of atoms and diatomic molecules particularly, which in turn furnishes the solid foundation upon which the theory rests.

In two recent papers in the *Physical Review*, Professor R. S. Mulliken has presented a valuable summary of the present status of the physicists valence theory as well as a discussion of his own viewpoint on the subject.[2] The pioneer work on valence from this angle was done by W. Heitler and F. London[3] who considered the particular case of the formation of H_2 from two hydrogen atoms, H+H, an example which is especially important be-

[1] Editor's Column, Physics **1**, 69 (1931).

[2] R. S. Mulliken, Phys. Rev. **40**, 55 (1932).

[3] W. Heitler and F. London, Zeits. f. Physik **44**, 455 (1927); F. London, "Quantentheorie und Chemische Bindung" in "Quantentheorie und Chemie, Leipziger Vorträge 1928." An English translation of these lectures has been announced.

cause it is the simplest case of a *homopolar* molecule; that is, one in which the constituents are definitely not oppositely charged ions. While the binding forces between ions have a clear enough origin in the electrostatic attractions of the constitutents, those acting between identical atoms are much more mysterious. The analysis of Heitler and London brought to light the origin of these forces and their relation to quantum theory and especially to the Pauli exclusion principle.

From the chemical point of view one of the most important factors leading to binding forces between molecules is the tendency of the electrons to form symmetrical groups or "shells" about the nuclei, a process analogous to the completion of a closed shell of an atom to form a rare gas structure. Thus in the formation of sodium fluoride (NaF) one can think of the valence electron of the sodium atom as going over to the fluorine atom, leaving both "ions" with the electronic configuration characteristic of the rare gas, neon. In addition to this process extensive use is also made of the idea of *shared* electrons, that is, electrons which do not properly belong to any one constituent of the molecule but which act like binders or *bonds* between two (or more) of the atoms.

It is instructive to consider how the problem can be studied from the point of view of wave mechanics. It is a sufficient approximation to the truth to consider that the atomic nuclei are all fixed in the equilibrium positions which they occupy within the molecule, and to neglect at first their vibratory motions. The electrons can be thought of as being like an electrical *cloud* surrounding and filling up the space between the nuclei. The density of this cloud is to be found in the usual manner by solving the Schrödinger equation and using the square of the modulus of the ψ-function as the density function. While this statement suffers from the defect that it considers the electron cloud as a 3-dimensional cloud instead of a cloud in the many-dimensional coordinate space of the electrons, it does bring out the important idea that generally speaking, *one cannot localize electrons on individual atoms, but must consider each electron as belonging to all of the nuclei.* Perhaps this is the most important single point involved in the physical theory of valence.

Since it is a bit inconvenient to think of an electron cloud in many-dimensional space, it has become customary, and is very useful, by making suitable approximations, to replace the single Schrödinger equation for say n electrons in the field of m nuclei by n separate equations, one for each electron. Each individual electron can then be considered as forming its own electrical cloud, which in general surrounds *all* of the nuclei. The electrical repulsion of the electrons is replaced by a specious sort of interaction among the various electron clouds. The interesting point about these electron clouds is that they can show a certain geometrical symmetry in space—a symmetry which is conditioned by the symmetry of the nuclear configuration (perhaps roughly tetrahedral as in the case of the methane molecule (CH_4) or pyramidal as in the ammonia molecule (NH_3)). Since the nuclei have positive electrical charges one might expect a kind of condensation of the clouds of negative electricity around them, so that the electron density would be largest in the immediate neighborhood of the nuclei, but that the electron clouds would also extend throughout the region between and surrounding the nuclei.

This way of speaking in terms of *electron clouds* and the like just as though an electron really were a continuous distribution of electricity instead of a discrete point charge is not in strict accordance with present-day interpretations of quantum mechanics, but nevertheless it is to be valued for the readiness with which it can be employed in interpreting the various steps in the more precise theory. Let us now point out some of these steps.

The modern picture of an atom is well known: a heavy positively charged nucleus around which electrons move, grouped in more or less definitely defined shells. In order to extract an electron from one of the inner shells considerable energy must be expended. while to remove one of the valence electrons from the outermost regions of the atom requires a much smaller expenditure of energy. Now imagine two or more atoms brought near together. Due to the mutual attractions and repulsions of the nuclei and the electrons, the valence electrons will be disturbed and may no longer stay on one atom, but may begin to travel around the molecule as a whole, becoming more or less free lances. The electrons in the lower shells will be less perturbed by the presence of the outer nuclei and will remain, for the most part, intact on their own

respective nuclei. However, this description is but another angle of our previous picture, for the electron shells around each nucleus are the analogs of the *condensation* of the electron clouds of which we spoke previously, while the valence electrons which encircle the nuclei form the *enclosing cloud* of negative electricity.

The aim of the physical theory of valence is substantially to combine these two associated sets of ideas into a single scheme which will have the principal advantages of both methods—the definiteness and clarity of the electron shell conception as well as the versatile vagueness of the electron cloud picture. It must of course be amplified further by the inclusion of the spin of the electron and the exclusion principle which we have neglected so far in this discussion.

ACCORDING to the ideas of Mulliken[2] and Hund,[4] the procedure to be adopted is about as follows: one assigns the individual wave functions for the electrons according to the rôle which the electrons are expected to play. For the electrons in the inner closed shells around the atoms one uses wave functions concentrated about the various nuclei. These are termed *atomic* wave functions or *atomic orbitals*. For the outer or valence electrons it is better to choose wave functions which are distributed over the molecule as a whole, these being termed *molecular orbitals*. The actual choice of the form for these non-localized wave functions depends upon the geometrical symmetry of the molecule (and its *electrical* symmetry also, of course) and also on the requirement that the energy of the normal state must be as low as possible. At this point the experience gained in dealing with diatomic molecules becomes of considerable value.

It is interesting to note the analogy of this procedure with the wave mechanical theory of metals.[5] In both cases one pays scant attention to the electrons in the inner closed shells of the *atoms*, but concentrates his attention on the few free electrons which pass rather easily around among all of the ions and throughout the whole region of the molecule or crystal as the case may be.

To pass from these simple considerations of bonding by means of the purely electrostatic action to the more complicated questions of electron pairing and even *anti-bonding* electrons, one must be much more precise in his use of the Pauli exclusion principle and the symmetry properties of the wave functions. One can no longer be content with allowing for interactions between the electrons by means of simple interactions between their associated "clouds"; one must bring in the actual exchange phenomenon and allow for the antisymmetry of the wave function with respect to an interchange of electrons.

It is at this point that one is in some doubt as to the best method of procedure. Just how is one to interpret such a thing as an *electron-pair bond?* Is it formed from two valence electrons originally coming from different atoms or could two electrons from the same atom form such a pair? Which is the more important aspect, the pairing of electrons or the tendency of the electrons to form larger groups and to go into *closed shells?*

Slater[6] and Pauling[7] have recently developed theories based primarily on the idea of valence electrons as localized on their parent atoms. The individual wave functions of these electrons lead to cloud distributions of striking forms[8] which are very suggestive of oriented bonds, so that it is easy to adopt the tempting hypothesis that the arrangements of bonds in the molecule can be correlated in a one-to-one manner with the possible arrangements of these oriented electron distributions, a notion which is in the closest agreement with the chemists picture of bonds as grapples which hook the atoms together. The Mulliken-Hund theory, on the other hand, is opposed to so rigid a correlation of the bonds with the individual atoms, but prefers instead to consider the bonds as belonging to the molecule or radical as a whole. This feature is accomplished by localizing the wave functions for the valence electrons on the whole molecule rather than on or between individual atoms.

So far as the pure quantum mechanical theory is concerned the distinction between

[4] F. Hund, Zeits. f. Physik **73,** 565 (1932).
[5] Editor's Column, Physics **1,** 271 (1931).
[6] J. C. Slater, Phys. Rev. **37,** 481 (1931); **38,** 325 and 1109 (1931).
[7] L. Pauling, Journ. Am. Chem. Soc. **53,** 1367 (1931).
[8] H. E. White, Phys. Rev. **38,** 513 (1931).

the two procedures is not really serious as probably neither method will fit all cases, and the truth lies somewhere between them. On the whole the physical picture of valence is in good qualitative agreement with the chemical picture, and it is to be hoped that a bold prosecution of the theory will result in a clearer picture of the meaning of valence and its quantitative determination.

E. L. HILL

AUTHOR INDEX TO VOLUME II

References with (EC) are from the Editor's Column

Asao, S. Photoelectric properties of thin films of alkali metals—12
Ambrose, H. A. (see Lawton, H. C.)—365

Baker, Edward B. and Robert F. James. Potential distribution, radiation and electrical conduction in paper—73
Bardeen, John (see Peters, Leo J.)—103
Botset, Holbrook G. and Paul Weaver. Radon content of soil gas—376
Buchta, J. W. Cosmic rays: what are they?—405 (EC)
Bull, Henry B. and Ross Aiken Gortner. Electrokinetic potentials. XI. Effect of sodium soaps on the electric moment of the double layer at an aqueous-cellulose interface—21

Cauer, W. New theory and design of wave filters—242
Compton, Karl T. New spectroscopy laboratory of the Massachusetts Institute of Technology—205
Culver, Charles A. Electrostatic alternator—448

Dehlinger, Walter. Ultra high-frequency oscillation of the magnetostatic vacuum tube—432

Ewing, W. Maurice (see Leet, L. Don)—160

Fox, Gerald W. and W. G. Hutton. Experimental study of parallel-cut piezoelectric quartz plates—443
Fruth, H. F. Cathode sputtering, a commercial application—280

Gortner, Ross Aiken (see Bull, Henry B.)—21

Hartley, Kenneth. New instrument for measuring very small differences in gravity—123
Hemingway, A. and J. F. McClendon. A.C. Wheatstone bridge for audio and radio-frequency measurements—396
Hergenrother, Rudolf C. Precision method of measuring small changes of lattice spacings of metal single crystals—63
——— X-ray spectrometer with stationary ion chamber—211
Hershberger, W. D. Multiple peaks in supersonic interferometry—269
Hill, E. L. Dissociation of molecules by electron impact—99 (EC)
——— Excitation of atomic mercury by electron impact—99 (EC)
——— Free rotation in molecules—403 (EC)
——— Interaction of light and matter—60 (EC)
——— Isotopes of hydrogen—60 (EC)
——— Neutron—310 (EC)
——— Neutron again—403 (EC)
——— Pauli exclusion principle—201 (EC)
——— Physical theory of valence—476 (EC)
——— Physics in the Soviet Union—309 (EC)
——— Quantum theory of radiation—101 (EC)
——— Velocity of sound in gases—200 (EC)
Ho, T. L. Speed, speed factor and power input of different designs of diffusion pumps, and remarks on measurements of speed—386
Houghten, F. C. (see Pugh, Emerson M.)—93
Houghton, H. G. Size and size distribution of fog particles—467
Hull, A. W. Electronic devices as aids to research—409
Hutton, W. G. (see Fox, Gerald W.)—443

Ingersoll, L. R. Geothermal gradient determinations in the Lake Superior copper mines—154

James, Robert F. (see Baker, Edward B.)—73
Jamison, Noel C. Cathode-ray frequency multiplier—217

Kersten, H. Influence of hydrogen ion concentration on the crystal structure of electrodeposited cobalt—274
——— Influence of temperature on the crystal structure of electrodeposited antimony—276

Lawton, H. C., H. A. Ambrose and A. G. Loomis. Chemical treatment of rotary drilling fluids—365
Leet, L. Don and W. Maurice Ewing. Velocity of elastic waves in granite—160
Loomis, A. G. (see Lawton, H. C.)—365

McClendon, J. F. (see Hemingway, A.)—396
McCollum, Burton and F. A. Snell. Asymmetry of sound velocity in stratified formations—174

Meara, Francis L. Magnetic susceptibility of some binary alloys—33
Morgan, S. O. (see White, A. H.)—313
Muskat, Morris. Potential distributions in large cylindrical disks with partially penetrating electrodes—329

Page, Leigh. Electromagnetic equations and systems of units—289
Peters, Leo J. and John Bardeen. Some aspects of electrical prospecting applied in locating oil structures—103
Phillips, C. J. Electron diffraction for classroom demonstration—48
Pugh, Emerson M. and F. C. Houghten. Heat waves through insulating walls—93

Rashevsky, N. Further studies on the theory of spontaneous dispersion of small liquid systems which are the seats of physico-chemical reactions —303
Reyerson, L. H. Attempt to activate adsorbed mercury atoms by ultraviolet light—70
Robinson, Denis M. Unpolarized resistivity of glass —52

Slotnick, M. M. Charts for torsion balance readings —131
Snell, F. A. (see McCollum, Burton)—174
Stedman, C. K. Thermionic frequency doubler—42
Stoops, W. N. Development of polar characteristics in insulating oils—322
Stuhlman, Otto, Jr. Mechanics of effervescence—457

Tonks, Lewi. Impedance characteristics of loaded Lecher systems—1

Van Orstrand, C. E. On the correlation of isogeothermal surfaces with the rock strata—139

Weaver, Paul (see Botset, Holbrook G.)—376
White, A. H. and S. O. Morgan. Dielectric properties of some glycols—313
Whitehead, J. B. Dielectric loss and relaxation time in rosin—82
Wilson, H. A. Calculation of the motion of the ground from seismograms—186
Woods, J. P. Calculation of detection performance for large signals—225

Zirbel, N. N. Effects of heat treatment on fine metallic suspensions—134

ANALYTIC SUBJECT INDEX TO VOLUME II

Alloys
Magnetic susceptibility, Francis L. Meara—33

Biophysics
Dispersion of small liquid systems, N. Rashevsky —303

Catalysts
An attempt to activate adsorbed mercury atoms by ultraviolet light, L. H. Reyerson—70
Conductivity, electrical (see Electrical conductivity and resistance)
Conductivity, thermal (see Thermal conductivity)
Crystals and crystal structure
Influence of *pH* on crystal structure, H. Kersten —274
Influence of temperature on the structure of electrodeposited antimony, H. Kersten—276
Measuring small changes of lattice spacings, Rudolf C. Hergenrother—63

Dielectrics and dielectric properties
Dielectric loss and relaxation time in rosin, J. B. Whitehead—82
Polar characteristics in insulating oils, W. N. Stoops—322
Properties of some glycols, 1 to 100 k.c., A. H. White, S. O. Morgan—313
Disperse systems
Theory of spontaneous dispersion of small liquid systems, N. Rashevsky—303
Drilling fluids
Chemical treatment of rotary drilling fluids, H. C. Lawton, H. A. Ambrose, A. G. Loomis—365

Editor's column
Cosmic rays: what are they? J. W. Buchta—405
Dissociation of molecules by electron impact, E. L. Hill—99
Excitation of atomic mercury by electron impact, E. L. Hill—99
Free rotation in molecules, E. L. Hill—403
Interaction of light and matter, E. L. Hill—60
Isotopes of hydrogen, E. L. Hill—60
Neutron, E. L. Hill—310
Neutron again, E. L. Hill—403
Pauli exclusion principle, E. L. Hill—201
Physical theory of valence, E. L. Hill—476
Physics in the Soviet Union, E. L. Hill—309
Quantum theory of radiation, E. L. Hill—101
Velocity of sound in gases, E. L. Hill—200

Effervescence
Mechanics of, Otto Stuhlman, Jr.—457
Elasticity
Velocity of waves in granite, L. Don Leet, W. Maurice Ewing—160
Electrical circuits
Calculation of detection performance for large signals, J. P. Woods—225
Characteristics of loaded Lecher systems, Lewi Tonks—1
Thermionic frequency doubler, C. K. Stedman—42
Wave filters, new theory and design, W. Cauer—242
Wheatstone bridge for audio and radio-frequency measurements, A. Hemingway, J. F. McClendon—396
Electrical conductivity and resistance
Potential distribution, radiation and electrical conduction in paper, Edward B. Baker, Robert F. James—73
Unpolarized resistivity of glass, Denis M. Robinson—52
Electrokinetic potentials
Effect of soaps on electric moment of double layer, Henry B. Bull, Ross Aiken Gortner—21
Electromagnetic theory (see also Electrostatics)
Systems of units, Leigh Page—289
Electron diffraction
Apparatus for classroom demonstration, C. J. Phillips—48
Electrostatics
Potential distributions in cylindrical disks with penetrating electrodes, Morris Muskat—329

Fogs
Size and distribution of particles, H. G. Houghton —467
Frequency multipliers
Cathode-ray type, Noel C. Jamison—217
Thermionic frequency doubler, C. K. Stedman—42

Geophysics
Asymmetry of sound velocity in stratified formations, Burton McCollum, F. A. Snell—174
Calculation of the motion of the ground from seismograms, H. A. Wilson—186
Charts for torsion balance readings, M. M. Slotnick—131

Geophysics—(continued)
Correlation of isogeothermal surfaces with rock strata, C. E. Van Orstrand—139
Electrical prospecting, Leo J. Peters, John Bardeen—103
Flow of fluids through sands into artesian wells, Morris Muskat—329
Geothermal gradient in Lake Superior copper mines, L. R. Ingersoll—154
Measuring small differences in gravity, Kenneth Hartley—123
Velocity of elastic waves in granite, L. Don Leet, W. Maurice Ewing—160

Geothermal data
Correlation of isogeothermal surfaces with rock strata, C. E. Van Orstrand—139
Geothermal gradient in Lake Superior copper mines, L. R. Ingersoll—154

Heat insulation (see Insulation)

Instruments and methods
Calculation of the motion of the ground from seismograms, H. A. Wilson—186
Cathode-ray frequency multiplier, Noel C. Jamison—217
Cathode sputtering. A commercial application, H. F. Fruth—280
Charts for torsion balance readings, M. M. Slotnick—131
Chemical treatment of rotary drilling fluids, H. C. Lawton, H. A. Ambrose, A. G. Loomis—365
Detection performance for large signals, J. P. Woods—225
Effects of heat treatment on metallic suspensions, N. N. Zirbel—134
Electrical prospecting, Leo J. Peters, John Bardeen—103
Electron diffraction for classroom demonstration, C. J. Phillips—48
Electronic devices, A. W. Hull—409
Electrostatic alternator; sine wave or special forms, Charles A. Culver—448
Measuring small changes of lattice spacings, Rudolf C. Hergenrother—63
Measuring small differences in gravity, Kenneth Hartley—123
Piezoelectric quartz plates, Gerald W. Fox, W. G. Hutton—443
Sensitivity of photoelectric cells, S. Asao—12
Speed, and power input of different designs of diffusion pumps, T. L. Ho—386
Wheatstone bridge for audio and radio-frequency, A. Hemingway, J. F. McClendon—396
X-ray spectrometer with stationary ion chamber, Rudolf C. Hergenrother—211

Insulation
Heat waves through insulating walls, Emerson M. Pugh, F. C. Houghten—93
Potential distribution, radiation and electrical conduction in paper, Edward B. Baker, Robert F. James—73

Laboratories
New spectroscopy laboratory of Massachusetts Inst. of Tech., Karl T. Compton—205

Lecher systems
Impedance characteristics, Lewi Tonks—1

Liquids
Mechanics of effervescence, Otto Stuhlman, Jr. —457

Magnetic properties
Susceptibility of some binary alloys, Francis L. Meara—33

Meteorology
Size and size distribution of fog particles, H. G. Houghton—467

Oscillators
Electrostatic alternator, Charles A. Culver—448
High-frequency oscillation of the magnetostatic tube, Walter Dehlinger—432
Piezoelectric, Gerald W. Fox, W. G. Hutton—443
Supersonic interferometry, W. D. Hershberger—269
Thermionic frequency doubler, C. K. Stedman—42

Photoelectric effect; cells
Properties of R—Ag—RO—Ag surfaces, S. Asao —12

Photometry
Potassium photoelectric cell, S. Asao—12

Piezoelectric effect
Parallel-cut quartz plates, Gerald W. Fox, W. G. Hutton—443

Prospecting
Electrical methods applied in locating oil structures, Leo J. Peters, John Bardeen—103

Radioactivity
Radon content of soil gas, Holbrook G. Botset, Paul Weaver—376

Resistance (see Electrical conductivity and resistance)

Seismograms
Calculation of the motion of the ground from seismograms, H. A. Wilson—186

Soils
Radon content of soil gas, Holbrook G. Botset, Paul Weaver—376

Sound (see Waves)

Sputtering
Commercial application, H. F. Fruth—280
Supersonics
Multiple peaks in supersonic interferometry, W. D. Hershberger—269
Suspensions
Effects of heat treatment, N. N. Zirbel—134

Thermal conductivity
Heat waves through insulating walls, Emerson M. Pugh, F. C. Houghten—93
Transformer oils
Development of polar characteristics, W. N. Stoops—322

Units
Electromagnetic equations and systems of units, Leigh Page—289

Vacuum pumps
Speed, and power input of different designs of diffusion pumps, T. L. Ho—386
Vacuum tubes
Aids to research, A. W. Hull—409
Cathode-ray frequency multiplier, Noel C. Jamison—217
Calculation of detection performance, J. P. Woods—225
High-frequency oscillation of the magnetostatic tube, Walter Dehlinger—432
Thermionic frequency doubler, C. K. Stedman—42
Use in electrostatic alternator, Charles A. Culver—448
Wave filters
New theory and design, W. Cauer—242
Waves
Asymmetry of sound velocity in stratified formations, Burton McCollum, F. A. Snell—174
Velocity of elastic waves in granite, L. Don Leet, W. Maurice Ewing—160
X-ray spectroscopy
Spectrometer with stationary ion chamber, Rudolf C. Hergenrother—211